REGISTERED No. M. 3121

UNIVERSITY
OF MICHIGAN
AUG 16 1956
PHYSICS
LIBRARY

PROCEEDINGS

OF THE

INDIAN ACADEMY OF SCIENCES

VOL. XLIII] *SECTION A* [No. 6

JUNE 1956

Price Rs. 2 or 3 Sh. *Annual Subscription Rs. 18*

THE PHYSICS OF CRYSTALS*

By Sir C. V. Raman

(*Memoir No. 85 of the Raman Research Institute, Bangalore 6*)

Received May 31, 1956

1. Introduction

It is the aim of this address to give a fresh orientation to the subject of crystal physics. We begin with a re-examination of the fundamental notions on which a theoretical approach to the problems of the subject has to be based. The ideas which emerge are then applied to find an answer to the following questions: What is the nature of the thermal agitation in crystals? What is the character of their vibration spectra? These questions are of fundamental importance since they confront us in any attempt to explain or interpret the physical behaviour of crystals. The results which emerge from our enquiry impinge on many aspects of crystal physics. But we shall restrict ourselves here to a consideration of those in which the relationships between theoretical reasoning and factual experience are most evident, *viz.*, the thermal properties of crystals and their spectroscopic behaviour. Even in these fields, we can here do no more than broadly indicate the general nature of the results which follow from the application of the new ideas.

2. The Theory of Einstein

It is appropriate that we begin with a reference to the classic paper of 1907 by Einstein introducing the quantum theory of specific heats, a paper which even fifty years after its publication remains worthy of careful study. Einstein commences his paper by showing that the acceptance of Planck's radiation formula demands as a necessary consequence that the energy of a resonator capable of absorbing or emitting radiation with a specific frequency can only increase or diminish by quanta proportional to that frequency. *It is inferred that the energy of any elementary structure capable of mechanical vibration should likewise obey the quantum rule.* Einstein then indicates a procedure which enables this principle to be applied to the case of crystals. He identifies the thermal energy of a crystal with the mechanical energy of vibration of an immense number of *individual* oscillators distributed over its volume, the total number of these oscillators being the same as thrice the number of atoms comprised in the crystal. It is assumed that

* Address to a Conference of Nobel Laureates at Lindau on the Lake of Constance, June 25th to 29th, 1956.

the oscillators could be grouped into sets; each set comprises a great number of individual oscillators characterised by a common frequency of vibration. The individual oscillators in each set occupy the various energy levels allowed by the quantum hypothesis for the particular frequency. The numbers occupying these levels are in the relative proportions determined by the respective energies and by the temperature as indicated by the principle of Boltzmann. The average energy of an oscillator in each of the sets is then evaluated. Summing up over all the oscillators in each of the sets, and then over all the sets, Einstein obtains an explicit formula for the thermal energy of the crystal as a function of the temperature.

Examining the procedure thus summarised, it is evident that every step in the argument can be justified. A crystal is an assembly of a great number of similar and similarly situated groups of atoms, the normal modes and frequencies of vibration of which would necessarily all be identical. The total number of degrees of dynamical freedom of the entire system may accordingly be divided up into sets, each set representing a great number of individual oscillators having a common frequency. Since these oscillators are interconnected, they can exchange energy with each other and thereby constitute a system in thermodynamic equilibrium of which the behaviour could be statistically described in terms of Boltzmann's principle. In other words, the procedure followed effects a synthesis of the results of classical dynamics with the notions of the quantum theory and the basic principles of thermodynamics. The simplicity of Einstein's theory is as noteworthy as its success in explaining the general character of the specific heat-temperature curve of crystals.

We conclude, therefore, that Einstein's approach to the problem is fundamentally correct. His theory indicates that the atomic vibration spectrum of a crystal would consist of a set of discrete monochromatic frequencies, their number being the same as the number of sets of oscillators which are the carriers of the thermal energy. By virtue of Boltzmann's principle, the distribution of this energy over the volume of the crystal would exhibit fluctuations both in space and in time, the magnitude of the fluctuations being the greater the higher the frequency of the oscillators under consideration. However, the theory as it stands gives no precise indication of how the oscillators in each set are to be enumerated and how their respective frequencies of vibration are to be determined. Neither is any indication given whether the modes of vibration of the solid recognised by the classical theory of elasticity have any place in the picture. We shall now proceed to show how these lacunæ in Einstein's theory may be filled up.

3. The Dynamics of Crystal Lattices

The fundamental role which the enumeration of the degrees of freedom of atomic movement plays in specific-heat theory derives its justification from the well-known theorem in classical mechanics regarding the small vibrations of a connected system of particles about their positions of equilibrium. This theorem states that all the possible oscillations of the system are superpositions of its normal modes of vibration in each of which all the particles of the system vibrate with the same frequency and in the same or opposite phases. On the other hand, in Einstein's theory we are concerned with the modes and frequencies of vibration of the *individual* oscillators of which the total number is equal to the number of degrees of dynamical freedom of the entire system. These two points of view can be reconciled by identifying the normal modes and frequencies of vibration which are characteristic of the structure of the crystal with those that describe the dynamical behaviour of the elementary units of which it is composed.

The fundamental property of crystal structure is that it comes into coincidence with itself following a unit translation along any one of the three axes of the lattice. Hence, the normal modes of vibration characteristic of the structure of a crystal should satisfy a similar requirement. This can evidently happen in two ways, *viz.*, the amplitudes and phases of oscillation of equivalent atoms in adjacent cells are the same; alternatively, the amplitudes are the same while the phases are all reversed following the unit translation. Since these two possibilities exist for each of the three axes of the lattice, we have $2\times2\times2$ or eight possible situations. In each of these situations, the equations of motion of the p atoms contained in the unit cell can be completely solved, yielding us $3p$ solutions. Thus in all, we have $24p$ solutions from which the three simple translations must be excluded. We are then left with $(24p-3)$ normal modes and frequencies of vibration. Thus, the fundamental result emerges that a crystal consisting of p interpenetrating Bravais lattices of atoms has $(24p-3)$ characteristic modes of vibration, each of which is characterised by a specific frequency. In $(3p-3)$ of these modes, equivalent atoms have the same amplitudes and phases of oscillation in the adjacent cells, while in the $21p$ other modes the amplitudes are the same, while the phases alternate in adjacent cells along one, two or all three of the axes of the lattice.

The $(24p-3)$ normal modes of vibration indicated by the preceding argument may obviously be regarded as the modes of internal vibration of the group of $8p$ atoms comprised in a supercell of the crystal lattice whose linear dimensions are twice as large as that of the unit cell containing p

atoms. The 3 omitted degrees of freedom would then represent the 3 degrees of translatory freedom of movement of the whole group of 8 p atoms included in the supercell. Thus, it emerges that the structural unit whose dynamical behaviour is representative of the entire crystal is not the unit cell of the crystal structure but is twice as large in each direction as the latter.

4. THE VIBRATION SPECTRUM OF A CRYSTAL

The considerations set forth above indicate that a crystal may be regarded as an assembly consisting of $(24p-3)$ sets of similar oscillators, each with its own distinctive vibrational frequency. Even a monatomic crystal for which $p = 1$ would have 21 characteristic frequencies, while a diatomic crystal for which $p = 2$ would have 45 and so forth. The number of distinct frequencies would however be reduced considerably if the crystal belongs to a class with a high degree of symmetry. For instance, it can be readily shown that a face-centred cubic lattice of atoms would have only four characteristic frequencies of vibration, while cubic crystals such as diamond and rock-salt having two non-equivalent atoms in the unit cell would each have nine distinctive frequencies. The important point to be emphasised is that the vibration spectrum of a crystal consists of a set of discrete monochromatic frequencies whose number is the greater, the more numerous the atoms included in its unit cell are or the lower the symmetry of the crystal.

To complete the picture, we have to consider the nature of the movements associated with the three omitted degrees of freedom representing the translatory movements of the supercell of the crystal lattice. Such translations would necessarily result in local stresses and strains of the same general nature as those contemplated in the theory of elasticity and hence would also give rise to localised oscillatory movements. In other words, to complete the picture of the thermal agitation envisaged in Einstein's theory, we have to superpose on the oscillations of precisely defined frequencies determined by the atomic structure of the crystal, other quantized oscillations whose frequencies are not so precisely defined, since they would depend upon the dimensions of the moving masses and the forces thereby brought into play. It is evident that the smaller the mass of the oscillators under consideration, the more numerous they would be and also the higher their frequencies of vibration. It follows that the spectrum of the thermal agitation represented by such movements would be continuous and would exhibit a concentration of frequencies most marked at the upper end of the frequency range and falling off rapidly to zero as we move towards the lower end of the range.

5. The Theories of Debye and Born

The views set forth above regarding the nature of the thermal agitation in crystals and the character of their atomic vibration spectra are essentially a justification and a development of the original ideas of Einstein outlined in his fundamental paper of 1907. It is a matter of scientific history, however, that an approach of an entirely different nature to the problems of crystal physics was put forward a few years later and found general acceptance. The reference here is to Debye's theory of specific heats familiar to all students of physics and chemistry and to the lattice dynamics of Born and his collaborators which is regarded with favour by the mathematical theorists. The theories of Debye and Born differ in detail, but the basic idea in both is the same, namely that we are here dealing with a boundary value problem in the theory of wave-propagation. Actually, what we are concerned with is the determination of the modes and frequencies of vibration of the atoms in a crystal about their positions of equilibrium. These modes and frequencies would be determined by the masses of the atoms and their interactions with the surrounding atoms in a domain the extent of which is limited by the range of the interatomic forces. It follows that considerations regarding wave-propagation and boundary conditions are not relevant to the problem.

A rigorous mathematical investigation of the theory of the propagation of waves in a general crystal consisting of p interpenetrating lattices of atoms on the basis of the classical mechanics shows that only in the limiting cases of the lowest frequencies of vibration is the group velocity of the waves identifiable with their phase velocity. With increasing frequency, the phase velocity and the group velocity diverge from each other, and the group velocity becomes zero for $(24\,p\text{-}3)$ distinct frequencies, the nature of the atomic modes of vibration for these frequencies being identical to the $(24\,p\text{–}3)$ normal modes of vibration of the structure of the crystal referred to earlier in this address. Thus, the investigation from the standpoint of the theory of wave-propagation and of classical mechanics leads to the same result, namely that these are the $(24\,p\text{–}3)$ characteristic modes and frequencies of vibration of the structural units of which the crystal is composed.

We may put the matter a little differently by saying that while Einstein's theory identifies the thermal energy of a crystal with the quantized vibrational energy of immense numbers of oscillators having identical frequencies, Born's lattice dynamics identifies it with the quantized energy of immense numbers of wave-motions whose frequencies are all different. The two approaches are clearly irreconcilable, since in the one case, the vibration spectrum of

the crystal consists of a set of discrete frequencies, while in the other, it is a continuous spectrum. That Born's approach to the specific heat problem is indefensible becomes evident when we remark that his " waves " are not normal modes and hence are incapable of enumeration.

6. THE THERMAL PROPERTIES OF CRYSTALS

We shall now consider the application of the ideas indicated in the present address to the interpretation of the physical behaviour of crystals. The thermal properties may be considered first, since the nature of the thermal agitation plays a leading role in relation to them.

A familiar fact of experience is the extreme slowness with which heat diffuses through a solid. On the other hand, elastic waves travel through a solid with a velocity of some thousands of metres per second. It would be a formidable problem to explain such a fundamental difference in behaviour, if one were to identify thermal energy with wave-motion, as is done in the theories of Debye and Born. Such a paradox does not however confront us on the present view of the nature of the thermal agitation in which it is identified with the energy of vibration of individual oscillators localised in the crystal. The conduction of heat through a solid would on this view be the result of an exchange of energy quanta between the individual oscillators. Such a process would bear no resemblance whatever to wave-propagation in the ordinary sense of the word.

The evaluation of the specific heats of crystals as a function of temperature reduces itself to the problem of determining the $(24\,p-3)$ characteristic frequencies of atomic vibration. When p is unity or a small integer, the $21\,p$ superlattice frequencies make important contributions to the thermal energy. When p is large, however, the $(3\,p-3)$ modes and frequencies of the unit cell reappear with only minor changes as superlattice modes and frequencies, and hence many of the latter could be identified with the former without sensible error in the calculation of the thermal energy; a considerable simplification thereby results. The thermal energy represented by the three translations of the supercell may be assumed to be proportional to the absolute temperature, except at the very lowest temperatures where its continuous spectrum of frequencies would have to be explicitly to be taken into consideration.

Crystals exhibit a surprising variety of behaviour in respect of the changes in their linear dimensions with rise or fall of temperature. The present view of the nature of thermal agitation which regards it as a localised vibration of individual oscillators opens a pathway to the interpretation of

the observed facts. The finite amplitudes of vibration of the individual oscillators and the mechanical anharmonicity associated therewith would result in the frequencies of vibration diminishing in the higher states of excitation. It would also result in a change of the average dimensions of the individual oscillators, which again would depend on the modes of vibration and hence may be very different in different directions. The integrated effect would be a shifting accompanied by a broadening of the lines in the vibration spectra and a change in the linear dimensions of the crystal. Thus, a close correlation is to be expected between the thermal expansion of crystals and the changes in their spectroscopic behaviour with rise or fall of temperature.

7. The Spectroscopic Behaviour of Crystals

The vibration spectra of crystals are accessible to experimental study with a great variety of materials and by diverse techniques of investigation. The nature of the spectra becomes manifest when the absorption of light by crystals exhibiting visible colour (*e.g.*, the inorganic chromates), or of ultra-violet light by crystals (*e.g.*, the aromatic organic compounds) is investigated with the crystals cooled down to the lowest possible temperatures. The absorption spectra then appear fully resolved into a set of sharply defined lines. These can be interpreted as combinations of the electronic with the vibrational frequencies of the crystal. Very low temperatures are also necessary for effecting a similar resolution into sharp lines of the luminescence spectra of various crystals of which such luminescence is an inherent property, *e.g.*, the uranyl salts and of other crystals of which the luminescence is ascribable to the presence of an impurity phosphor (*e.g.*, ruby). Such luminescent crystals also exhibit at low temperatures characteristic absorption spectra which are resolved into discrete lines and which are related by an approximate mirror image symmetry to their emission spectra.

There are also other and rather more direct methods of investigation. Three different techniques based on infra-red spectroscopy are available, *viz.*, the emission, absorption and reflection of infra-red radiations by crystals. In these techniques, the disturbing effects of thermal agitation and of the anharmonicity of the vibrating electric doublets in the crystal are strongly manifested. Nevertheless, by an appropriate choice of the material to be investigated and of the techniques used, *e.g.*, by varying the thickness of the crystal, cooling it to low temperatures and the application of adequate resolving power, it is possible to obtain results capable of unequivocal interpretation. Finally, we have the method based on the study of the scattering

of light in crystals. The results obtained by this method are of such importance that they will be considered separately in the next section.

The whole body of experimental evidence forthcoming with the materials and methods described above confirms the thesis that apart from disturbing effects such as those mentioned earlier, the atomic vibrations in crystals appear as a set of sharply defined monochromatic frequencies in the spectrum.

8. THE SCATTERING OF LIGHT IN CRYSTALS

The nature of the results to be expected when a crystal is traversed by an intense monochromatic beam of light is different in relation to the $(3p-3)$ modes of atomic vibration which have the same phase in adjoining cells of the lattice, and the $21p$ modes in which the phases are opposite in adjoining cells along one, two or all three of the axes of the lattice. In either case, we are concerned with the scattered radiations having their origin in the changes of optical polarisability of the vibrating atomic groups. Ordinarily, except in the cases where the symmetry of the vibrational modes results in there being no resultant change of optical polarisability, the $(3p-3)$ modes would manifest themselves as frequency shifts in the spectrum of the scattered light. On the other hand in the $21p$ modes, the optical moments being in opposite phases in adjoining cells, their effects would cancel out. However, if the amplitudes of vibration are sufficient, the changes in optical polarisability proportional to the squares of the atomic displacements would also have to be considered. It is then possible for all of the $(24p-3)$ modes of atomic vibration to appear with doubled frequency shifts in the spectrum of the scattered light. The intensity of such scattering, being proportional to the square of the absolute atomic displacements, would necessarily be small. Strongly exposed spectrograms would accordingly be necessary to record the same.

It is evident that the study of the second-order spectra of light-scattering is of the greatest importance, since in the first place they allow us to observe and measure the frequencies of modes which do not appear in the first-order spectrum, and secondly because the intensity of the lines of the second-order spectra relative to those of the first-order spectra is a measure of the absolute magnitude of the interatomic displacements responsible for the changes in optical polarisability. Studies of this kind are obviously most suitably undertaken with crystals of relatively simple structures, as for example, diamond, rock-salt, calcite and quartz, since the results are then most readily interpreted.

Very detailed investigations of the kind indicated carried out at Bangalore have established that the vibration spectra of crystals include both the $(3p-3)$ and the $21p$ modes with discrete monochromatic frequencies, and further that the oscillators whose vibrations manifest themselves as frequency shifts are of the same order of magnitude in their dimensions as the unit cells of the crystal structure. The latter result is inferrable from the fact that the relative intensity of the first- and the second-order spectra is of the same order of magnitude in crystals as in fluids. For, the size of the quantized oscillators emitting the scattered radiation of any given frequency determines the absolute magnitude of the interatomic displacements responsible for the variations of optical polarisability.

Summary

1. Einstein's view of a crystal as an assembly of immense numbers of quantized oscillators having a common set of vibration frequencies is not only the logical and correct view of the matter but also proves itself when fully developed to be an eminently successful view. It gives us a deep and quantitative insight into the thermal behaviour of solids. The nature of the vibration spectra of crystals indicated by it is confirmed in detail by the results of spectroscopic studies with diverse materials and by various techniques and with especial completeness by studies on the diffusion of light in crystals.

2. The ideas underlying the specific-heat theories of Debye and Born are irreconcilable with the observed spectroscopic behaviour of crystals and especially with the effects exhibited in their second-order spectra of light-scattering.

ON THE INTENSITY AND POLARISATION OF THE LIGHT FROM THE SKY DURING TWILIGHT—PART II

By J. V. Dave
(*Physical Research Laboratory, Ahmedabad-9*)

Received April 12, 1956
(Communicated by Professor K. R. Ramanathan, F.A.SC.)

I. Introduction

In a recent paper,[1] observations of the intensity and polarisation of the light from the sky during twilight taken at Mount Abu during 1951 were presented and briefly discussed. It was shown that for depressions of the sun exceeding 7° or 8°, the zenith sky was much brighter than would be expected if primary scattering alone were responsible for the light and that in the treatment of twilight problems, due account should be taken of the contributions from secondary scattering, as has been shown by Hulburt.[2] Marked discontinuities in the polarisation of the light from the zenith sky at solar depressions of 5°, 8°, 12° and 17° support the presence in twilight of other contributions in addition to primary scattered light.

1.1. *Summary of previous work*

Robley[3] has recently given a method of calculating the intensity and polarisation of the secondary (multiply) scattered light during twilight. His work is based on the work of Dr. S. Chandrasekhar[4] for an infinite plane-parallel atmosphere of defined optical thickness. To compute the secondary scattered radiation for the zenith sky for a solar depression D, Robley extends the atmospheric path traversed by the solar rays to a vertical plane in the atmosphere passing through the centre of the earth and making an angle D/2 with the observer's vertical. He then calculates the scattered light emanating from this plane in a direction parallel to the observer's horizon, with certain simplifying assumptions which lead to a constant value of 50% for the polarisation of the secondary scattered light from the zenith sky throughout the period of twilight. *Prima facie*, this does not appear to be correct, because observation shows that with increasing values of solar depression, the brightness of the sky becomes more and more concentrated towards the horizon in the sun's meridian plane.

1.2. *General outline of the method adopted in this paper*

The method adopted in this paper for the calculation of secondary scattering is based on the work of Chapman and Hammad.[5,6] The following assumptions were made:—

(1) The earth was taken to be a uniform sphere of radius 6370 km., surrounded by an exponential atmosphere of equivalent scale height 7 km.

(2) The atmosphere was arbitrarily divided into a number of concentric shells of 4 km. thickness, for computing the intensities of primary and secondary scattered radiations.

(3) The solar radiation falling on the top of the atmosphere was assumed to be unpolarised and its intensity taken to be unity.

(4) The depolarisation factor d of air due to molecular anisotropy was taken to be 0·04.

(5) Higher orders of scattering than secondary were neglected.

(6) No correction was made for the absorption or scattering of light by dust or haze.

(7) Atmospheric refraction was neglected.

(8) No correction was made for reflection by the ground.

II. Theory

In Fig. 1, ABC represents a section of the earth; O is its centre and a its radius. R_0 is the position of the observer on the surface of the earth. OR_0 represents the direction of the observer's zenith. Q is a point in the atmosphere in the direction of observation R_0Q. The Z-axis is chosen to lie along the observer's zenith OR_0. The X-axis lies in the plane of the paper such that the XOZ plane is parallel to the incident solar radiation. The Y-axis is perpendicular to the plane of paper passing through O. The polar co-ordinates (θ, ϕ) of a given direction are such that θ is the angle which the direction makes with the Z-axis, and ϕ is the azimuth with XOZ as the reference plane. With this convention, the polar co-ordinates of the incident solar radiation SP are (Z_0, O). If the direction of observation is the zenith or R_0Q, its θ, ϕ are (O, O). PQ the direction of primary scattered radiation is given by (θ', ϕ'). The unit vectors along SP, QR_0 and PQ are denoted respectively by s, k and k'.

2.1. *Intensity of primary scattered radiation*

Consider a solar beam of intensity I_∞ travelling along SP. I_∞ denotes the intensity of solar radiation outside the earth's atmosphere in a specified narrow wave band, being the energy received per unit time on unit area normal to the vector s. Let σ denote the mass coefficient of scattering and ρ the density of air at a distance s from P along PS.

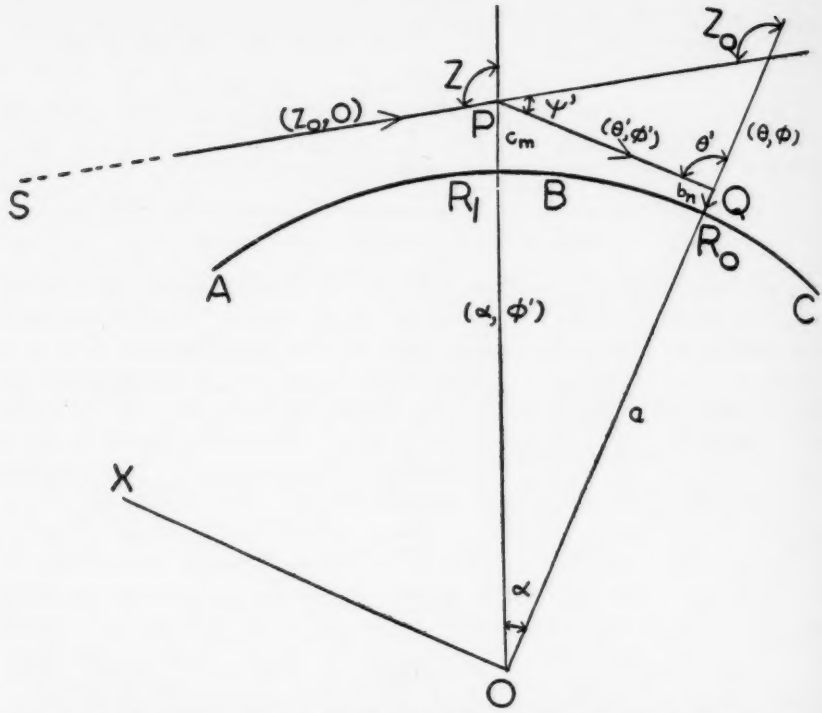

FIG. 1. The incident light is primarily scattered at P (where the local zenith angle of the sun is Z, and the height $R_1P = c_m$). The direction PQ is defined by (θ', ϕ'). The direction of observation towards the observer's zenith is defined by $\theta = 0$, $\phi = 0$. The primary scattered light travelling along PQ gets rescattered at Q along QR_0 towards the observer. $QR_0 = b_n$.

Then

$$\int_{\infty}^{P} \sigma . \rho . ds = \tau_{SP} \tag{1}$$

is the equivalent optical path which the solar radiation has to travel in the earth's atmosphere before reaching P. It will be shown later that τ_{SP} is a function of the vertical height c_m of P above the surface of the earth and of the local zenith angle (Z) of the sun at P. The intensity of the solar radiation at P is then given by

$$I = I_{\infty} e^{-\tau_{SP}} \tag{2}$$

Let PQ (θ', ϕ') be a direction along which the incident solar radiation is scattered from P according to the Rayleigh law of scattering. The energy

scattered from P in a cone of small solid angle dk' with apex at P is given by

$$E_1\,dk' = \frac{3\sigma I_\infty}{16\pi(1+\frac{1}{2}d)}\,e^{-\tau_{sp}}(1+\cos^2\psi'+d\sin^2\psi')\,dk' \quad (3)$$

where d is the depolarisation factor due to molecular anisotropy and ψ' the angle between s and k' given by

$$\cos\psi' = \cos Z_0\cos\theta' + \sin Z_0\sin\theta'\cos\phi' \quad (4)$$

This scattered radiation is polarised and can be resolved into two beams of plane polarised light at right angles to each other. If $E_{1n'}$ represents the primary scattered emission from P in the direction of k' with its electric vibration along the vector n' perpendicular to the plane sk' at P, and $E_{1t'}$, the intensity of the radiation with its electric vector along t' perpendicular to n', we have

$$E_{1n'} = \frac{3\sigma I_\infty}{16\pi(1+\frac{1}{2}d)}\,e^{-\tau_{sp}} \quad (5)$$

and

$$E_{1t'} = KE_{1n'} \quad (6)$$

where

$$K = d + (1-d)\cos^2\psi' \quad (7)$$

Consider a small surface area dS at Q perpendicular to PQ. The amount of primary scattered radiation from P passing through dS per second is given by

$$E_{1n'}(1+K)\,e^{-\tau_{PQ}} \times \frac{dS}{s^2}$$

where dS/s^2 is the solid angle subtended by dS at P and τ_{PQ} the equivalent optical path from P to Q. It will be later shown that τ_{PQ} which is given by

$$\tau_{PQ} = \int_P^Q \sigma.\rho.ds$$

is a function of θ', c_m and b_n. If dV is a small volume element surrounding P and subtending a small solid angle dk' at dS, and if ρ' is the density at P, then the amount of primary scattered radiation passing through dS per second from a mass element $\rho'.dV$ surrounding P is given by

$$E_{1n'}(1+K)\,e^{-\tau_{PQ}}\frac{dS}{s^2}\rho'.dV$$

and the intensities $R_{1n'}$ and $R_{1t'}$ of the normal and transverse components of primary scattered radiation passing normally through unit area at Q through unit solid angle along k' is given by

$$R_{1n'} = \int_{Q}^{\infty} E_{1n'}\, e^{-\tau_{PQ}} \frac{dS}{s^2} \times \frac{\rho' \cdot dV}{dS \cdot dk'}$$

and

$$R_{1t'} = K R_{1n'}$$

the integration extending from ∞ to Q when the whole path is illuminated by solar rays, or upto the shadow limit when a part of PQ lies in the shadow region of the earth.

Substituting the values of $E_{1n'}$ and of $dV = s^2 . ds . dk'$ in $R_{1n'}$, we have

$$R_{1n'} = \frac{3\sigma I_{\infty}}{16\pi (1 + \frac{1}{2}d)} \int_{Q}^{\infty} e^{-\tau_{SP}} e^{-\tau_{PQ}} \rho' . ds \tag{8}$$

and

$$R_{1t'} = K R_{1n'} \tag{9}$$

It must be noted that unlike the plane-parallel atmosphere, cos Z on the actual earth changes along QP and also with ϕ'. Hence τ_{SP} is not independent of ϕ'. Thus the integration formulæ developed by Chapman and Hammad for $R_{1n'}$ are not applicable in this and we have adopted numerical integration.

2.2. *Intensity of secondary scattered radiation*

Having obtained the values of $R_{1n'}$ and $R_{1t'}$ for different values of θ' and ϕ' at Q, the next problem is to consider the effective contribution by the volume element at Q towards the secondary scattered radiation travelling along QR_0. Let n be the unit vector perpendicular to the $k'k$ plane at Q. If E_{2n} and E_{2t} are defined as the energy of the secondary emission for normal and transverse components emitted at Q respectively, then as shown by Hammad, we have

$$E_{2n} = \frac{3\sigma}{16\pi (1 + \frac{1}{2}d)} \int \{A_1 + K A_2\} R_{1n'}\, dk'$$

and

$$E_{2t} = \frac{3\sigma}{16\pi (1 + \frac{1}{2}d)} \int \{B_1 + K B_2\} R_{1n'}\, dk'$$

where

$$\left.\begin{aligned} A_1 &= d + 2(1-d)\cos^2 \chi_{nn'} \\ A_2 &= d + 2(1-d)\cos^2 \chi_{nt'} \\ B_1 &= d + 2(1-d)\cos^2 \chi_{tn'} \\ B_2 &= d + 2(1-d)\cos^2 \chi_{tt'} \end{aligned}\right\} \tag{10}$$

$\chi_{nn'}$, $\chi_{nt'}$, $\chi_{tn'}$ and $\chi_{tt'}$ are respectively the angles between the vectors n and n', n and t', t and n' and t and t' and the formulæ for obtaining their values are as given by Hammad.

$$\cos \chi_{nn'} = \cos(\xi - \xi') \tag{11}$$

$$\cos \chi_{nt'} = \cos \psi' \sin(\xi - \xi') \tag{12}$$

$$\cos \chi_{tn'} = \cos \psi \sin(\xi' - \xi) \tag{13}$$

$$\cos \chi_{tt'} = \sin \psi \sin \psi' + \cos \psi \cos \psi' \cos(\xi' - \xi) \tag{14}$$

where ψ, ψ', ξ and ξ' are defined by the equations

$$\cos \psi = \cos Z_0 \cos \theta + \sin Z_0 \sin \theta \cos \phi \tag{15}$$

and

$$\sin \xi = \frac{\sin \theta \sin \phi}{\sin \psi} \tag{16}$$

Since $dk' = \sin \theta' . d\theta' . d\phi'$, the equations for E_{2n} and E_{2t} can be re-written as

$$E_{2n} = \frac{3\sigma}{16\pi(1 + \frac{1}{2}d)} \iint \{A_1 + KA_2\} R_{1n'} \sin \theta' . d\theta' . d\phi' \tag{17}$$

and

$$E_{2t} = \frac{3\sigma}{16\pi(1 + \frac{1}{2}d)} \iint \{B_1 + KB_2\} R_{1n'} \sin \theta' . d\theta' . d\phi' \tag{18}$$

Knowing E_{2n} and E_{2t} for a number of points along QR_0, the tota secondary scattered radiation received at R_0 along QR_0, can be integrated. Its normal and transverse components R_{2n} and R_{2t} are given by

$$R_{2n} = \int_{R_0}^{\infty} E_{2n} e^{-\tau_{QR_0}} \rho . ds \tag{19}$$

and

$$R_{2t} = \int_{R_0}^{\infty} E_{2t}\, e^{-\tau_{QR_0}} \rho . ds \tag{20}$$

where ρ is the density of air at Q and τ_{QR_0} is the equivalent optical path from Q to R_0. It is a function of b_n as well as of θ.

III. TABLES FOR COMPUTING THE SECONDARY SCATTERED RADIATION

The quantities required for computing $R_{1n'}$ by the summation method such as s, Δs, τ_{SP}, have been tabulated by many workers such as Sekera,[7] Chapman[8,9] and others. However, their tabulation could not easily fit into our system, and all the quantities required for this work were therefore tabulated from the formulæ given below.

As already mentioned in 1.2, the atmosphere is arbitrarily divided into a number of concentric layers of 4 km. thickness. The base of the nth layer is at a height of $4(n-1)$ km. while its centre is at $(4n-2)$ km. The positions of Q are selected at the base of the different layers, and of P at the centres of the successive layers. On replacing the integral of Equation (8) by a sum, we have

$$R_{1n'} = \frac{3\sigma\rho_0 I_\infty}{16\pi(1+\frac{1}{2}d)} \sum e^{-\tau_{SP}} e^{-\tau_{PQ}} e^{-c_m/H} \Delta s \qquad (21)$$

$\rho' = \rho_0 e^{-c_m/H}$ for an exponential atmosphere and H the equivalent scale height is assumed to have a uniform value of 7 km.

If the values of τ_{SP}, τ_{PQ} at the centres of the different layers and also of Δs the thickness of the layers for any θ' are known, $R_{1n'}$ can be calculated. Since τ_{SP} is a function of Z and c_m, we have to calculate for a given position of Q and a fixed value of Z_0, the local zenith angle Z of the sun at the centres of the successive layers along QP. For this, it is necessary to tabulate a shown in Fig. 1 for different values of c_m.

3.1. s, *the distance of the centre of the layer from the base of another layer in any direction*

From Fig. 1, we have

$$(a+c_m)^2 = s^2 + (a+b_n)^2 + 2s(a+b_n)\cos\theta'$$

On neglecting c_m^2 and b_n^2 in comparison with the other terms,

$$s^2 + 2s(a+b_n)\cos\theta' - 2a(c_m - b_n) = 0 \qquad (22)$$

With the help of Equation (22), the values of s were tabulated for different values of c_m and $\theta' = 0°$, 15°, 30°, 45°, 60°, 75°, 80°, 85°, 88° and 90° when the position of Q is at b_1, the ground level. From this table, it is easy to obtain the values of s corresponding to any b_n and θ' between 0° and 90° with sufficient accuracy. For positions of Q above the ground, when θ' can take values greater than 90°, QP can intercept some of the lower layers twice. This was appropriately allowed for in computing the path lengths for θ' between 90° and 180° at similar intervals. It is expected that the

tabulated values of s are correct within 1 km. when s is small and within 2 km. when it is large.

3.2. Δs, *thickness of the layer in any direction*

Equation (22) was used to calculate the distance Δs between the bases of two consecutive layers for all the above-mentioned values of θ'. $\text{Log}_e \Delta s$ was tabulated for all values of c_m, b_n and θ' required in the calculation.

3.3. *Z, the local zenith distance of the sun for any position of P for a given* Z_0

In Fig. 1, the vertical through P (PR_1O) makes an angle α with the Z-axis. It can be represented by (α, ϕ') and Z is given by

$$\cos Z = \cos Z_0 \cos \alpha + \sin Z_0 \sin \alpha \cos \phi' \tag{23}$$

α can be determined from the relation

$$\sin \alpha = \frac{s}{a + c_m} \sin \theta' \tag{24}$$

The values of $\sin \alpha$ and $\cos \alpha$ were tabulated for all the positions mentioned in 3.1 and used for the other similar positions as necessary.

When Z is greater than 90°, there is a limit below which P would not be illuminated by direct sunlight. Limiting values of $\cos Z$ for different values of c_m can be obtained from

$$\sin Z_s = \frac{a}{a + c_m} \tag{25}$$

With the help of Equation (24) tables of $\cos Z$ were prepared for Z_0 corresponding to 90°, 94°, 98°, 102° and 106° for all the values of θ' and b_n and at intervals of 15° for ϕ'.

3.4. τ_{SP}, *the equivalent optical path from outside the atmosphere to the point P which is at a height* c_m *above ground and for different values of cos Z*

Consider a point P situated at a height c_m in its vertical above the surface of the earth. Let the incident solar radiation make an angle Z with OP (Fig. 2). Let P′ be any point in SP, at a distance s from P and at a vertical height h from the ground. The density at P′ is given by

$$\rho = \rho_0 e^{-h/H}$$

and the equivalent optical path $\tau_{SP}(\cos Z, c_m)$ as defined by (1) is given by

$$\tau_{SP}(\cos Z, c_m) = \sigma\rho_0 \int_{\infty}^{P} e^{-h/H}\, ds \tag{26}$$

$$\sigma\rho_0 = \frac{8\pi^3}{3\lambda^4} \times \frac{(n_0^2 - 1)^2}{N_0} \times \frac{6(1 + d)}{6 - 7d} \tag{27}$$

where

λ = wave-length of the incident radiation

n_0 = refractive index of the air

N_0 = number of molecules per c.c. at the ground

ρ_0 = density of the air in gm. per c.c. at the ground.

From Fig. 2, we have,

$$(a + h)^2 = s^2 + (a + c_m)^2 + 2s\,(a + c_m) \cos Z$$

and neglecting c_m^2 and h^2 compared to the other terms, we have,

$$h = \frac{s^2}{2a} + \frac{(a + c_m) \cos Z}{a} s + c_m$$

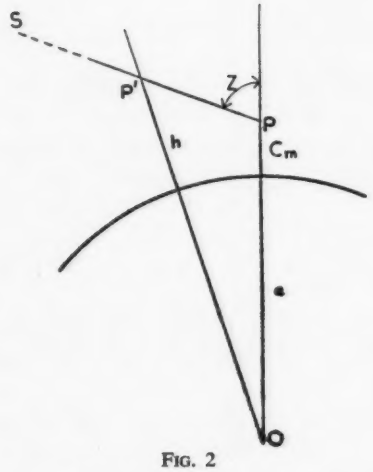

FIG. 2

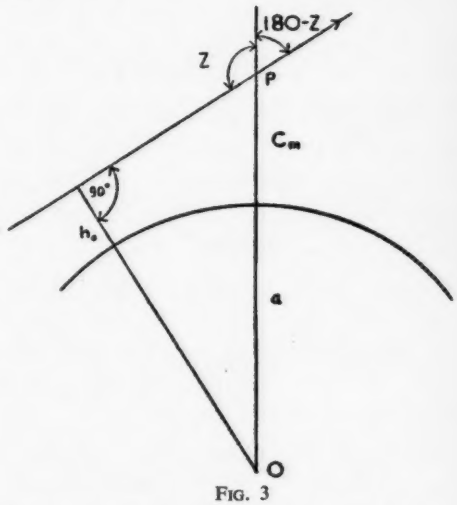

FIG. 3

On substituting this in Equation (26) and carrying out the integration, we have

$$\tau_{SP}(\cos Z, c_m) = \sigma\rho_0 \sqrt{\frac{\pi a H}{2}} e^{-c_m/H} \times e^{\frac{(a+c_m)^2 \cos^2 Z}{2aH}} \left[1 - Erf\left\{\frac{(a + c_m) \cos Z}{\sqrt{2aH}}\right\}\right] \qquad (28)$$

The function $Erf(y)$ is tabulated in books of *Mathematical Tables* at regular intervals between 0 and 3 while for $y > 3$, we can use the standard expansion formula. It can be shown that for $\cos Z = 1$ and $c_m = 0$, Equation (28) reduces to

$$\tau_{SP}(1, 0) = \sigma\rho_0 H = \tau_1$$
$$= \text{the vertical optical path} \qquad (29)$$

After substituting $\sigma\rho_0$ by τ_1/H in Equation (28), the equation was used to tabulate $\tau_{SP}(\cos Z, O)/\tau_1$ for a number of intervals of $\cos Z$ between 0 and 1. From this, we can calculate τ_{SP} for any wave-length by selecting τ_1. The intervals are sufficiently numerous to obtain τ_{SP}/τ_1 for any $\cos Z$ within the accuracy required. For positive values of $\cos Z$ and c_m, $e^{-c_m/H}$ is the most important factor and

$$\tau_{SP}(\cos Z, c_m)/\tau_1 = \tau_{SP}(\cos Z, O)\, e^{-c_m/H}/\tau_1 \qquad (30)$$

For negative values of $\cos Z$, the following method is used. From Fig. 3,

$$\frac{a + h_0}{a + c_m} = \sin Z$$

from which h_0 can be calculated for a given Z and c_m. Then

$$\frac{\tau_{SP}(\cos Z, c_m)}{\tau_1} = \frac{2\tau_{SP}(O, O)}{\tau_1} e^{-h/H} - \frac{\tau_{SP}\{\cos(180 - Z), c_m\}}{\tau_1} \qquad (31)$$

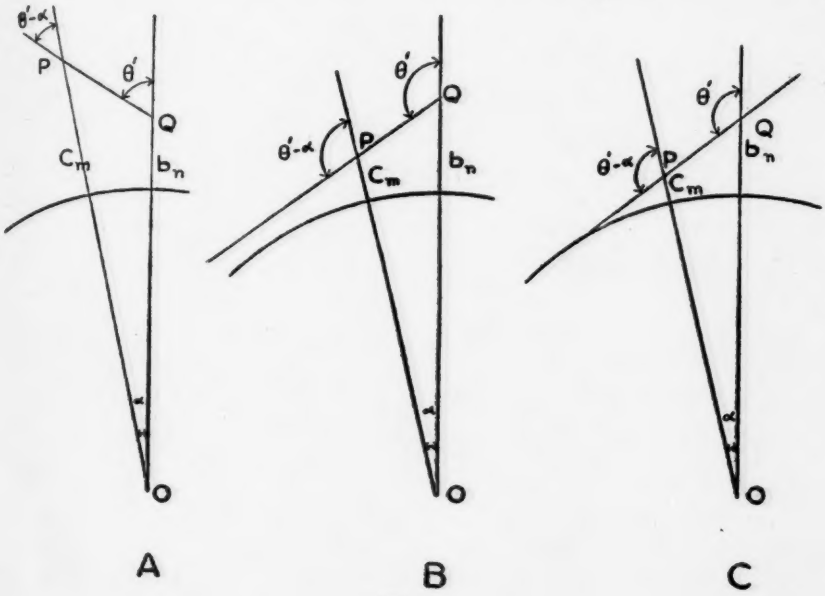

FIG. 4

Using Equation (31), $\tau_{SP}(\cos Z, c_m)/\tau_1$ were tabulated at regular intervals from zero to the shadow limit for different values of c_m from c_1 to c_{18}. For higher values of c_m the calculations were carried out whenever necessary.

3.5. τ_{PQ}, *equivalent optical path between any two points in the atmosphere*

From Figs. 4 A and B, we can write

$$\frac{\tau_{PQ}(\cos\theta', c_m \text{ to } b_n)}{\tau_1} = \frac{\tau_{SP}(\cos\theta', b_n)}{\tau_1} - \frac{\tau_{SP}\{\cos(\theta' - \alpha), c_m\}}{\tau_1} \quad (32)$$

For negative values of θ', for which PQ intersects the surface of the earth, the calculation of τ_{PQ} is similar to that indicated in Fig. 4 C.

IV. INTENSITY AND POLARISATION OF THE ZENITH SKY

In this section the results of the computation of the intensity and polarisation of the primary and secondary radiations from the zenith sky during twilight for $\tau_1 = 0{\cdot}2$ corresponding to $\lambda = 4350$ A are given. The effect of adding a fixed intensity of night air-glow radiation with a polarisation of 4% as obtained from twilight observations is then discussed.

4.1. $R_{1n'}$, *primary scattered radiation received from any direction for different values of* Z_0

$R_{1n'}$ was calculated with the help of Equation (21). The summation extends over all the layers which lie in the sunlit part of the atmosphere. I_∞ was taken to be equal to unity, and $\sigma\rho_0 = \tau_1/H$ from Equation (29). Equation (21) shows that the part $e^{-\tau_{PQ}} e^{-c_m/H} \Delta s$ is independent of ϕ' and Z_0. An auxiliary table of $\{-\tau_{PQ} - c_m/H + \text{Log}_e \Delta s\}$. for different values of b_n and $\tau_1 = 0{\cdot}2$ was prepared to reduce the work of computation.

When $R_{1n'}$ was computed for different values of θ' and ϕ', for $Z_0 = 90°$ and $b_n = b_1$ or b_2, it was noticed that for a fixed θ', the graph of $R_{1n'}$ against $\cos\phi'$ was nearly a straight line for values of θ' between 0° to 75° and between 100° to 180° (Fig. 5). It was slightly curved when θ' lay between 75° and 95°. Therefore, $R_{1n'}$ was obtained by linear interpolation after computing its value for $\cos\phi' = 1{\cdot}0, 0{\cdot}5, 0{\cdot}0, -0{\cdot}5$ and $-1{\cdot}0$ for a given b_n. This procedure was adopted when Z_0 was 90° and 94° and the whole sky more or less illuminated by direct solar radiation. For higher values of Z_0, $R_{1n'}$ was calculated individually for each ϕ' and θ' as only a small portion of the sky could then get direct sunshine.

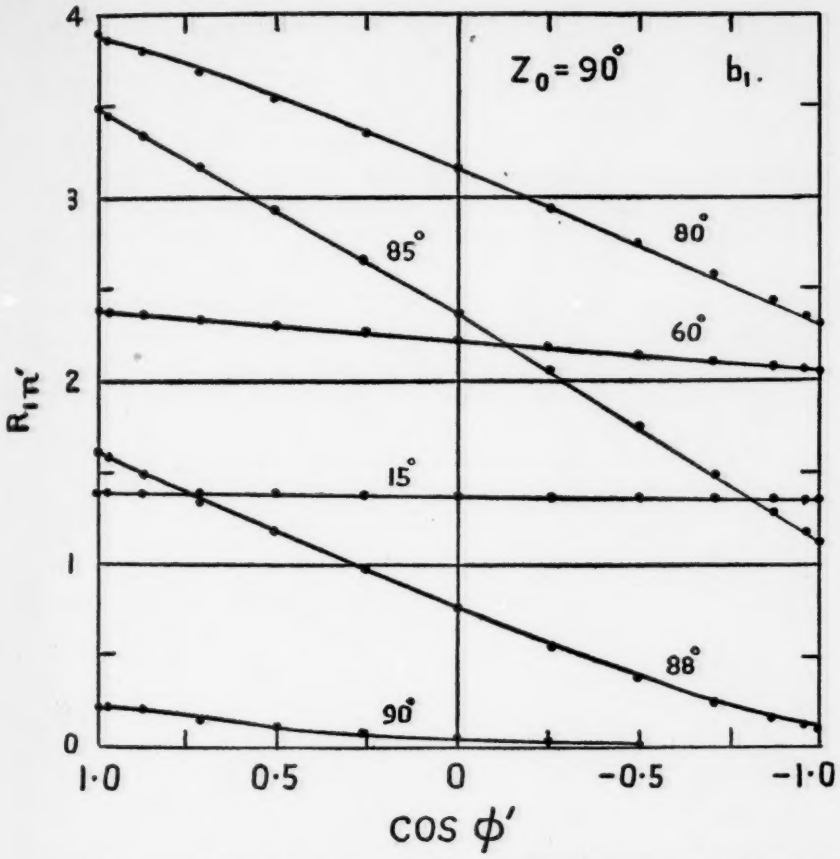

FIG. 5. Variation of the normal component of primary scattered light ($R_{1n'}$) with solar azimuth (cos ϕ') for different zenith angles of the sky from 15° to 90° as seen by an observer at ground level ($b_1 = 0$ km.). The sun is assumed to be on the observer's horizon ($Z_0 = 90°$).

The variation of the normal component of primary scattered radiation as received by the observer at the ground from different parts of the sky for Z_0 from 90° to 102° is shown in Fig. 6.

4.2. *E_{2n} and E_{2t}: Secondary emission from any point in the direction of observation*

Equation (17) can be rewritten as

$$\rho_0 E_{2n} = \frac{3\sigma\rho_0}{16\pi(1+\frac{1}{2}d)} \sum\sum [\{A_1+KA_2\} R_{1n} d\phi'] \sin\theta' . d\theta'$$

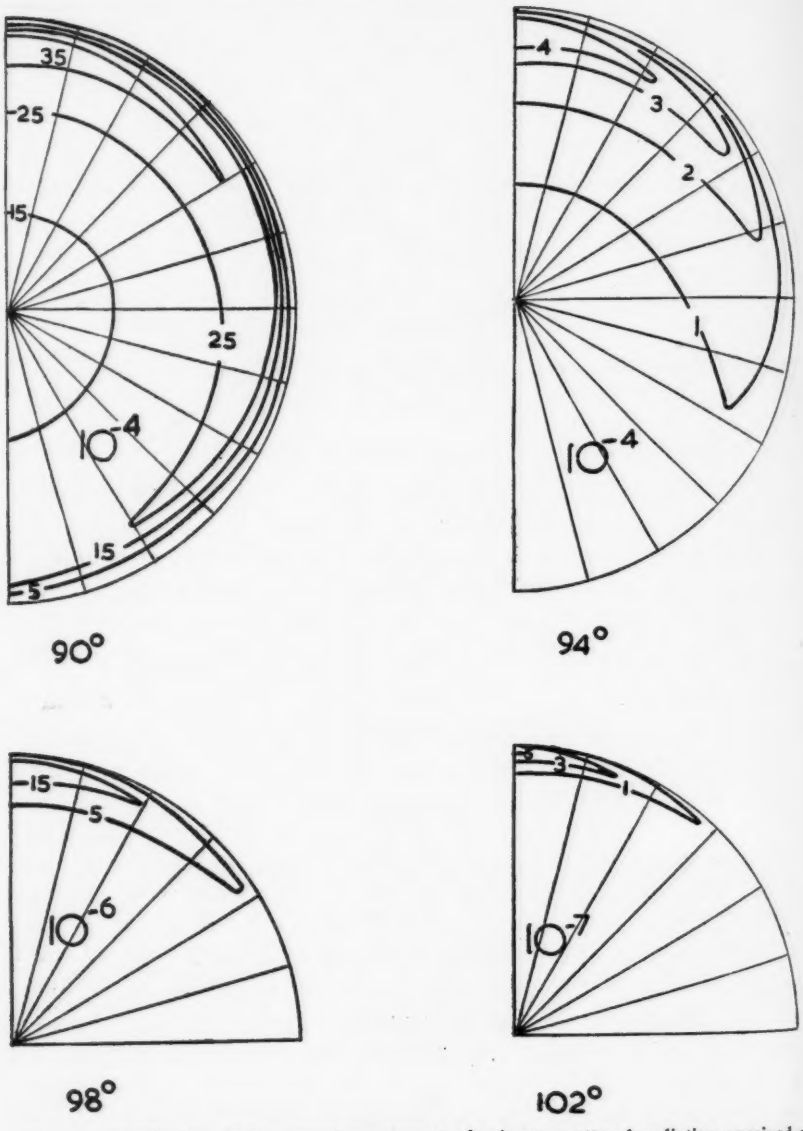

FIG. 6. Distribution of the normal component of primary scattered radiation received at the ground from different parts of the sky.

Knowing the values of $\{A_1 + KA_2\}$ and $R_{1n'}$ at definite intervals of θ' and ϕ' for different values of b_n and Z_0, further calculation was carried out in the following manner:

First, summation was carried out over ϕ', keeping θ' constant. $R_{1n'}$ was multiplied by the corresponding $\{A_1 + KA_2\}$, the arithmetic means of the consecutive products were then added and the sum multiplied by $d\phi' = 0{\cdot}5237$ radians corresponding to 30° interval. Symmetry about the principal plane gives the value for 30° from the tabulated values for 15° intervals.

For summation over θ', $\Sigma[\{A_1 + KA_2\} R_{1n'} d\phi']$ was multiplied by the corresponding value of sin θ', and the arithmetic means of consecutive terms were taken. $R_{1n'}$ includes the exponential $\exp(-\tau_{SP} - \tau_{PQ})$. These were then multiplied by corresponding intervals of $d\theta'$ in radians. The summation of the product multiplied by $3\sigma\rho_0/16\pi(1 + \frac{1}{2}d)$ gave the value of $\rho_0 E_{2n}$ for the particular level b_n and Z_0 under consideration. The values of $\rho_0 E_{2n}$ and $\rho_0 E_{2t}$ so obtained are given in Table I for different values of b_n and Z_0.

TABLE I

$\rho_0 E_{2n}$ for the observer's zenith for different values of b_n *and* Z_0

b_n \ Z_0	90°	94°	98°	102°	106°
b_1	$0{\cdot}245\times10^{-4}$	$0{\cdot}143\times10^{-5}$	$0{\cdot}015\times10^{-6}$	$0{\cdot}013\times10^{-8}$	$0{\cdot}000\times10^{-10}$
b_2	0·339	0·199	0·032	0·051	0·025
b_3	0·445	0·262	0·062	0·133	0·117
b_4	0·535	0·326	0·101	0·287	0·383
b_5	0·584	0·406	0·162	0·605	1·037
b_6	0·587	0·491	0·237	1·040	1·994
b_7			0·295	1·389	2·769
b_8			0·311	1·507	3·048
	$\rho_0 E_{2t}$ for the observer's zenith for different values of b_n and Z_0				
b_1	$0{\cdot}077\times10^{-4}$	$0{\cdot}044\times10^{-5}$	$0{\cdot}004\times10^{-6}$	$0{\cdot}002\times10^{-8}$	$0{\cdot}000\times10^{-10}$
b_2	0·113	0·062	0·008	0·008	0·003
b_3	0·156	0·082	0·014	0·021	0·013
b_4	0·193	0·105	0·022	0·046	0·045
b_5	0·214	0·132	0·036	0·096	0·125
b_6	0·216	0·162	0·053	0·167	0·244
b_7			0·066	0·225	0·340
b_8			0·071	0·247	0·383

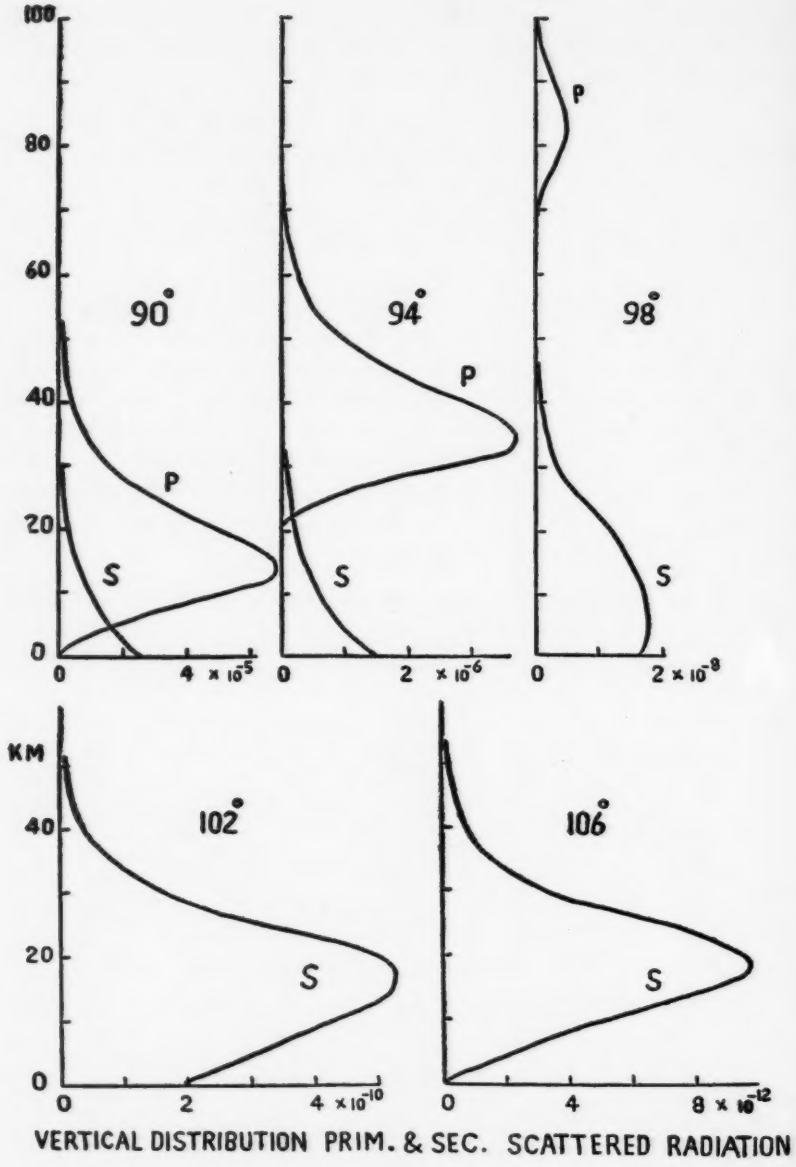

FIG. 7. Vertical distribution of primary and secondary scattered light from the zenith sky during twilight for solar zenith angles from 90° to 106°.

It will be seen from Table I that the computation has been stopped at b_6 for 90° and 94°. For heights greater than b_6, the value corresponding to b_6 has been used. A similar remark applies to heights greater than b_8 for 98°, 102° and 106°. This is justifiable because at these heights, the density becomes relatively small and the effective contribution to the light received by the observer becomes negligible (see Fig. 7).

4.3. *R_{2n} and R_{2t}: Normal and transverse components of the total secondary scattered light as received by the observer at the ground from his zenith*

Equation (19) can be rewritten as

$$R_{2n} = \Sigma \rho_0 E_{2n} e^{-\tau_{QR_0}} e^{-C_m/H} \Delta s \tag{33}$$

the summation extending over all the layers above the point of observation. $\Delta s = 4$ km. for $\theta = 0°$, $\phi = 0°$. τ_{QR_0} is the same as τ_{PQ} for $\theta' = 0°$ and $b_n = b_1$ when the observer is situated at ground level and the direction of observation is along his zenith. The value of $\rho_0 E_{2n}$ is the arithmetic mean of two successive values of b_n given in Table I. The vertical distribution of primary and secondary scattered radiation from the zenith sky for different solar angles are plotted in Fig. 7.

The values of R_{2n} and R_{2t} are given in Table II along with R_{1n}, R_{1t}, P_1 and P_2 where P_1, P_2 are the percentage polarisations of primary and secondary scattered light. P is defined by

$$P = \frac{R_n - R_t}{R_n + R_t} \times 100 \tag{34}$$

TABLE II

Intensity and polarisation of the primary and secondary scattered radiations from the zenith sky

Z_0	R_{1n}	R_{1t}	P_1 %	R_{2n}	R_{2t}	P_2 %
90	$1{\cdot}30\times10^{-3}$	$0{\cdot}052\times10^{-3}$	92·3	$2{\cdot}43\times10^{-4}$	$0{\cdot}84\times10^{-4}$	49
94	$6{\cdot}93\times10^{-5}$	$0{\cdot}31\times10^{-5}$	91·4	$1{\cdot}52\times10^{-5}$	$0{\cdot}48\times10^{-5}$	52
98	$9{\cdot}0\times10^{-8}$	$0{\cdot}5\times10^{-8}$	89	$4{\cdot}13\times10^{-7}$	$0{\cdot}94\times10^{-7}$	63
102	..	..	..	$1{\cdot}26\times10^{-8}$	$0{\cdot}20\times10^{-8}$	72
106	..	..	..	$1{\cdot}95\times10^{-10}$	$0{\cdot}24\times10^{-10}$	78

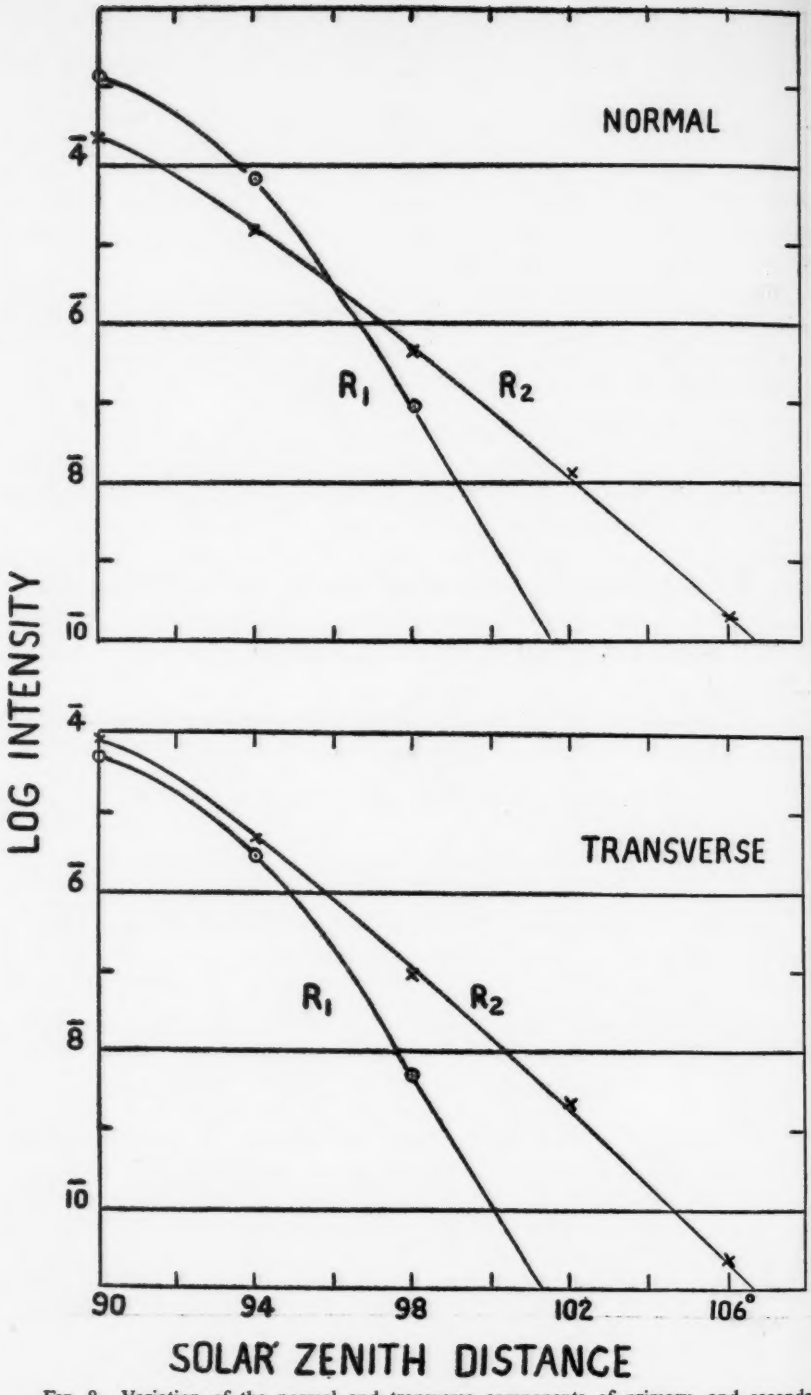

FIG. 8. Variation of the normal and transverse components of primary and secondary scattered light from the zenith sky during twilight.

4.4. *Variation of the intensity and polarisation of the zenith sky during twilight*

Figure 8 gives the variation of R_{1n}, R_{1t}, R_{2n} and R_{2t} with Z_0. Smooth curves were drawn from the values given in Table II and from them, the values were read out at each 1° interval to calculate the intensities and polarisations of the zenith sky at different zenith angles of the sun.

Figure 9 shows the variation with Z_0, of (*a*) the primary scattered radiation R_1, (*b*) the primary and secondary scattered radiations together, $R_1 + R_2$, (*c*) $R_1 + R_2 + R_0$ when R_0 is the background night air-glow radiation assumed to be constant at $1{\cdot}92 \times 10^{-9}$ and (*d*) the observed intensity

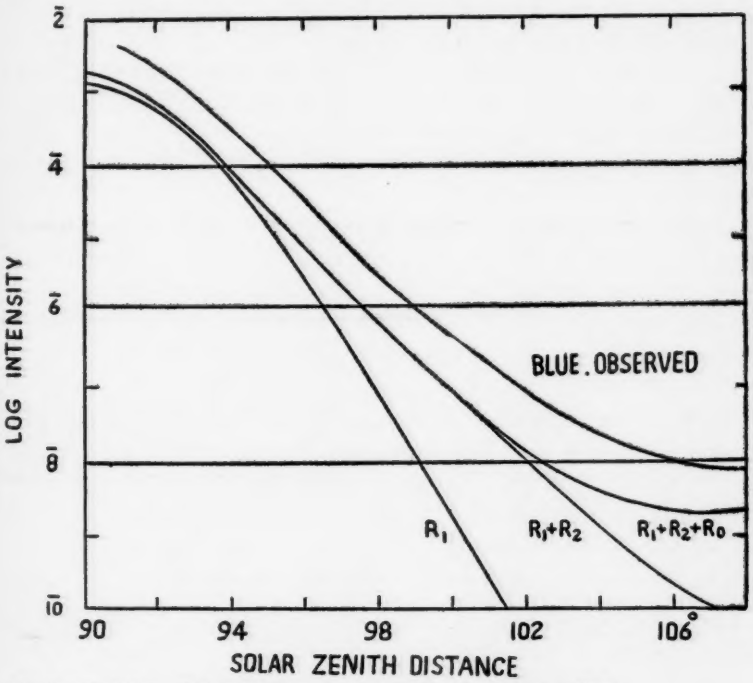

FIG. 9. Variation of the intensity of the zenith sky during twilight.

R_1 .. Primary scattering alone.

$R_1 + R_2$ .. Primary *plus* secondary scattering.

$R_1 + R_2 + R_0$.. $R_1 + R_2$ *plus* background night air-glow of constant intensity.

of the zenith sky for $\lambda = 4{,}500$ A during evening twilight as observed at Mount Abu. The magnitude of R_0 was fixed from observations of the zenith sky when the sun was more than 18° below the horizon.

It can be seen from the figure that the secondary scattered radiation becomes more and more important after 95°. Between 98° and 102°, the light received by the observer is mainly secondary scattered radiation. Afterwards, the night air-glow becomes comparable in intensity to secondary scattered light, and by 106°, practically only night sky emission remains as the factor contributing to the zenith sky intensity.

In Fig. 10 are given the curves of polarisation of the zenith sky when the different contributions are considered singly or jointly. The curve giving the polarisation of the primary scattered light shows that it is 92% at sunset and decreases to 88% at 100°. On the contrary, S representing the polarisation of the secondary scattered light shows an increase from 48% at sunset to 79% at 106°. Adding the normal and transverse components of the two radiations from the zenith sky and calculating the effective polarisation, the polarisation gets reduced to 84% at sunset. After 94°, the secondary scattered radiation becomes relatively more important and the polarisation shows a rapid fall; after 98°, P becomes unimportant and P + S follows S.

If night sky radiation of intensities $R_{0n} = 1{\cdot}00 \times 10^{-9}$ and $R_{0t} = 0{\cdot}92 \times 10^{-9}$ be added to $R_{1n} + R_{2n}$ and $R_{1t} + R_{2t}$ respectively, and the polarisation recalculated (Curve P + S + N), the curve gradually changes its course when the zenith distance of the sun increases beyond 99°, and the change becomes rapid after 102°. When Z is greater than 108°, night conditions get fully established.

When the calculated polarisation curve is compared with that obtained by observation, it is seen that while there is agreement in general features, there are some important differences. The observed values of polarisation are markedly smaller. The transitions are sharper in the observed curve than in the calculated one.*

This is probably due to the following causes:—

(1) The effect of dust in the atmosphere and of tertiary and higher orders of scattering have been neglected. Inclusion of these in the calculation will decrease the polarisation.

(2) The density of the atmosphere has been assumed to decrease exponentially with height with a scale height of 7 km. Actually, there are well marked stratifications in the atmosphere and the decrease of density with height is not a simple exponential. The difference

* Recent observations of polarisation at Mount Abu with a better type of polaroid have shown 80% polarisation at sunset and 55 to 60% between 8 and 12° solar depression.

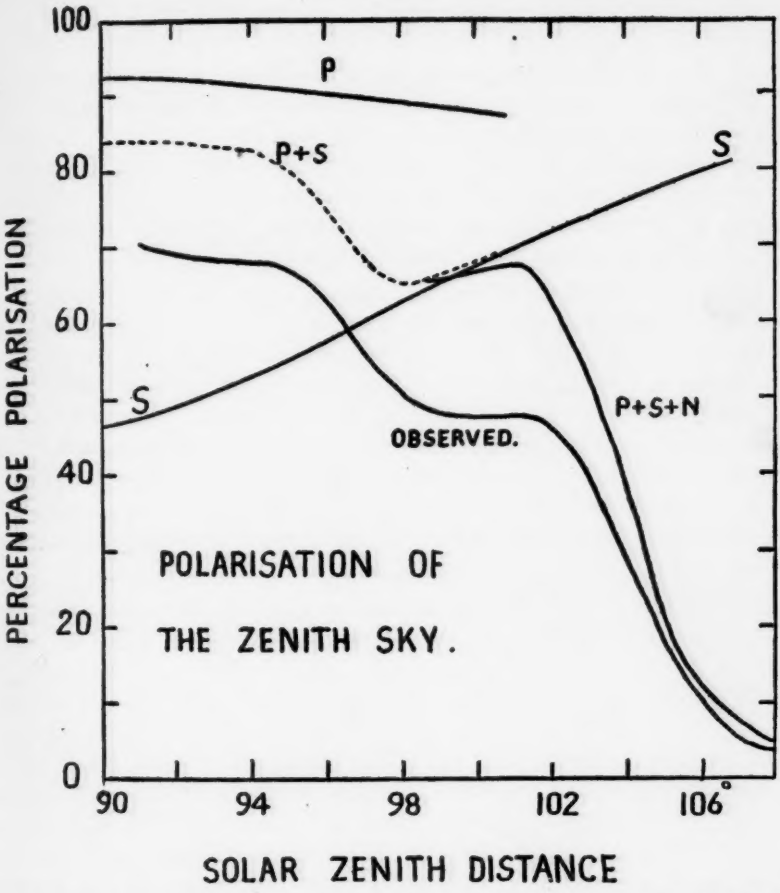

FIG. 10. Polarisation of the zenith sky during twilight for different zenith distances of the sun.

P	..	Percentage polarisation of primary scattered light.
S	..	Percentage polarisation of secondary scattered light.
P + S	..	Effective percentage polarisation of primary *plus* secondary scattered light.
P + S + N	..	Total effective polarisation when night air-glow of constant intensity and 4% polarisation is added to primary *plus* secondary scattered light.
Observed	..	Observed zenith sky polarisation at Mount Abu.

between the courses of the observed and calculated curves between 94° and 98° can be related to the existence of the warm ozone layer between 30 and 60 km. An attempt is being made to remedy these defects in the theory.

V. POLARISATION OF THE SKY AT POINTS 30° FROM THE ZENITH AND IN THE PRINCIPAL PLANE OF THE SUN

In Part I, we also presented the observations of polarisation during twilight from two directions in the sky other than zenith, (1) at 30° from the zenith on the sunside $\theta = 30°$, $\phi = 0°$ and (2) at 30° from the zenith on the anti-sunside, $\theta = 30°$, $\phi = 180°$. These curves while showing the general features of the zenith polarisation curve, show some differences. In order to understand this, calculations have also been made of the polarisation in these two directions. They are plotted in Fig. 11.

The polarisation curves for the sunside show that the polarisation of primary scattered light (P) increases with Z_0 and so also the polarisation of secondary scattered light (S). However, the secondary scattered radiation is polarised to a much smaller extent than the primary and hence the resultant polarisation P + S, increases with Z_0 in the beginning when the primary scattered radiation is prominent and decreases afterwards when $Z_0 = 94{\cdot}5°$. For $Z_0 = 100°$, the primary scattered radiation is negligible and P + S practically coincides with S. On adding the night sky radiation, the P + S curve deviates from the S curve at 100°, and by 102° a sharp fall occurs.

On the anti-sun side, the polarisation of P shows a fall with Z_0 and the rate of increase of S is much smaller than on the side of the sun. This causes a slight fall of polarisation in the beginning and a comparative flat region between 98° and 102°.

VI. SUMMARY

The formulæ for the intensity of the secondary scattered light from the sky as developed by Chapman and Hammad for a plane-parallel infinite atmosphere of defined optical thickness have been modified so as to deal with the twilight problem in which the curvature of the atmosphere is of fundamental importance. Calculations have been made of the intensity and polarisation of the light received from the zenith sky for different values of the sun's zenith distance from 90° to 107° and for a radiation for which the optical thickness of the atmosphere is 0·2. For 0° to 5° solar depression, the primary scattering is predominant; as the angle increases, the secondary scattered light becomes more and more important and when the sun's depression is 8° to 12°, it is the principal contributing factor. Afterwards, the night air-glow becomes comparable in intensity and when the solar depression is 17° to 18°, only the air-glow radiation remains. The calculated values of intensity and polarisation are compared with the observational data collected at Mount Abu.

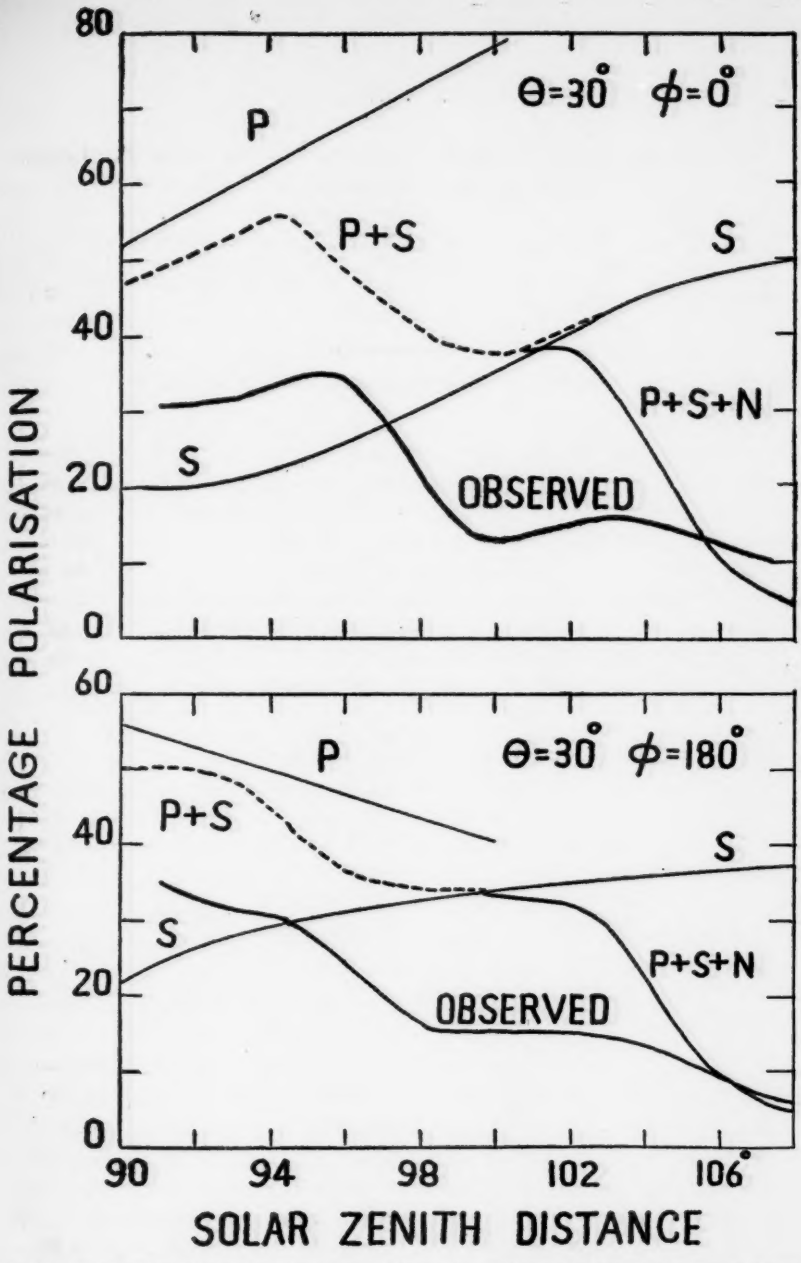

FIG. 11. Polarisation of the sky at points 30° from the zenith in the principal plane of the sun.

P	..	Percentage polarisation of primary scattered light.
S	..	Percentage polarisation of secondary scattered light.
P + S	..	Effective percentage polarisation of primary *plus* secondary scattered light.
P + S + N	..	Total effective percentage polarisation when night air-glow of constant intensity and 4% polarisation is added to primary *plus* secondary scattered light.
Observed	..	Observed sky polarisation at Mount Abu.

The author is grateful to the Council of Scientific and Industrial Research for the award of a Research Assistantship during the course of this study. He acknowledges with pleasure the help given by Shri V. L. Bhatt, M.Sc., in preparing some of the diagrams. Finally, the author takes this opportunity to express his indebtedness to Prof. K. R. Ramanathan, for suggesting the problem and valuable guidance.

REFERENCES

1. Dave, J. V. and Ramanathan, K. R. — *Proc. Ind. Acad. Sci.*, 1956, **43 A**, 67.
2. Hulburt, E. O. .. *Journ. Opt. Soc. America*, 1938, **28**, 227.
3. Robley, R. .. *Annales de Geophysique*, 1952, **8**, 1.
4. Chandrasekhar, S. .. *Radiative Transfer*, The International Series of Monographs on Physics, Clarendon Press, Oxford, 1950.
5. Hammad, A. and Chapman, S. .. *Phil. Mag.*, 1939, **28**, 99.
6. Hammad, A. .. *Astrophys. Journ.*, 1948, **108**, 338.
7. Link, F. and Sekera, Z. .. *Publ. Obs. Nat., Prague*, 1940, **14**, 1.
8. Chapman, S. .. *Proc. Phys. Soc.*, 1931, **43**, 483.
9. ———— .. *Ibid.*, 1953, **66 B**, 710.

MINERALOGY OF SOME INDIAN CLAYS*

By M. Ramakrishna Rao

(National Metallurgical Laboratory, Jamshedpur, India)

Received April 3, 1956

(Communicated by Sir C. V. Raman)

Abstract

Mineralogical compositions of five Indian clays have been determined by the petrographic, X-ray, electron-microscopic and differential thermal analysis methods. The relative importance of the methods is discussed and the procedures are described.

Introduction

A study of the mineralogical composition of five samples of Indian clays, used in the ceramic and refractory industries, has been made. The importance of such a study lies in the fact that to a large extent the working properties of the clays depend on their mineralogical composition, degree of crystallinity and grain size.

To determine the mineralogical composition of the clays, techniques complementary to one another, are generally required. As the grain size of most clay minerals is of the order of a few microns or less, the petrographic microscope does not have sufficient resolving power to distinguish the individual crystals. However, if the crystal size is coarse enough, as is the case with some dickites and kaolinites, the petrographic microscope can be used for their identification. On the other hand, it is possible to distinguish various types of clay minerals by X-ray diffraction procedures. The chief limitation of the X-ray method is that it is often difficult or impossible to detect impurities present in amounts less than 5% of the total material. It is here that the petrographic microscope has an advantage over the X-ray diffraction method.

The electron microscope has been of great help in determining the morphology, degree of crystallinity and grain size, which aid in distinguishing the clay minerals. Differential thermal analysis has been of great value for the study of clay minerals, but here also, it is not always possible to detect small percentages of impurities present in the clays. In the present paper, the results are given of a correlated study using the above techniques.

* This investigation was made by the author as part of his work on a Colombo Plan Fellowship at the Physical and Crystal Chemistry Section, Mineral Dressing and Process Metallurgy Division, Mines Branch, Department of Mines and Technical Surveys, Ottawa, Canada.

EQUIPMENT AND PROCEDURES

Petrographic Study

The clays were examined under a petrographic microscope by the powder method, using Shillaber's oils of known refractive indices. The samples were examined as received and also after washing away the finer and lighter fractions.

Electron Microscopic Study

An R.C.A. electron microscope of the electromagnetic type was used in this study. The fine clay suspensions were mounted on " formvar " films by standard procedures. The strength of the " formvar " solution used was 0·1% in dichloro-ethane. The films were shadowed by chromium evaporation *in vacuo*. The samples were examined at an initial magnification of 10,000.

Differential Thermal Analysis

Differential thermal analysis equipment has been described by many workers with some variation in details.[1] A brief description of the experimental arrangement used in the present work is detailed below. Sketches of the palladium block specimen holder are shown in Fig. 1.

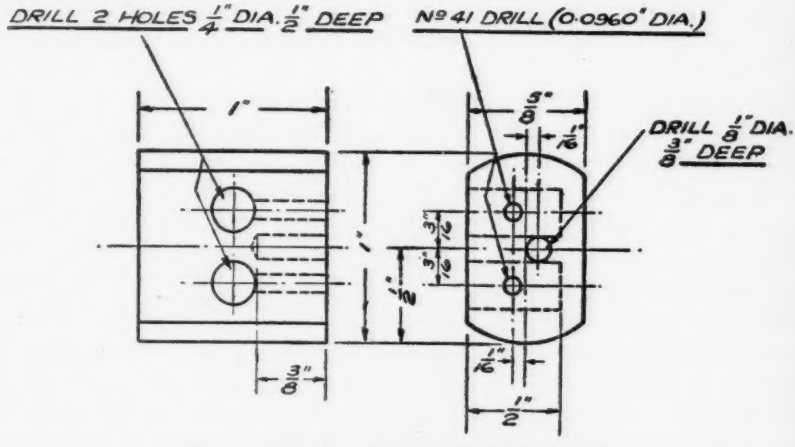

FIG. 1. Palladium Specimen Holder for D.T.A.

The sample under study is placed in a cavity in the specimen holder and an inert reference material, calcined alumina, is placed in another cavity. Two connected thermocouples are placed one in each cavity and the leads of this differential couple are connected to a preamplifier and then to a Leeds

and Northrup Recorder. Another thermocouple is placed in a separate cavity close to the specimens. The leads of this couplé are connected to a Leeds and Northrup Program Controller. The horizontal tube furnace carrying the specimen holder is now heated at the rate of 12° C. per minute. The rate of temperature rise is controlled by the Program Controller. The inert material in the palladium block is stable throughout the heating range, whereas the clay sample undergoes a succession of endothermic or exothermic reactions during heating. This results in the setting up of differential e.m.f.s which are recorded on the Leeds and Northrup Recorder, appearing as peaks on either side of the centre line of a strip chart. However, as soon as each reaction is over the temperature of the specimen equalises with that of the inert material, and the differential thermocouple record returns to the centre of the strip chart.

X-Ray Diffraction

X-ray examination was carried out by the powder diffraction techniques using North American Philips Co. high angle goniometer. The technique is described in detail by Klug and Alexander.[2] The salient features are as follows:

An X-ray beam impinges on the smooth surface of a finely pulverised specimen mounted in a rotating sample holder. The diffracted X-ray beam is picked up by a Geiger-Muller counter, scanning at a rate of $2\theta = 1°$ per minute, amplified and recorded on a moving chart from which θ values can be obtained and hence the corresponding *d*-spacings.

Results

X-Ray Diffraction

The results of X-ray examination of these five clays are given in Table I. Filtered Cu K radiation was used throughout. The *d*-spacings in Angstrom units are given for each clay. By comparison of the values with those in the A.S.T.M. Card Index of Powder Diffraction Patterns and also the available lieterature,[3] each set of the lines was attributed to a specific mineral constituent. The intensities of the kaolinite and mica lines showed some variations from those given by some of the previous workers. However, this could be expected, as the clays and micas do tend to exhibit preferred orientation. The intensities are estimated approximately from the magnitude of the peaks. Quartz, even when present in small amounts, gives much stronger peaks than kaolinite as, for instance, in the Rajhara and Jabbalpur clays. In such cases the strongest peak of the kaolinite is taken as 100, with which other peaks of lower intensities are compared, while the quartz lines of higher intensity are denoted as " very strong". The X-ray diffraction patterns of these clays are

TABLE I

X-Ray Diffraction Data on Indian Clays

Travancore-China Clay[1]			Chaibasa Clay[2]			Orissa Clay[3]			Jubbalpur Clay[4]			Rajhara Clay[5]		
I	*d*	Mineral	I	*d*	Mineral	I	*d*	Mineral	I	*d*	Mineral	I	*d*	Mineral
100	7·155	Kaolinite	100	7·166	Kaolinite	100	7·144	Kaolinite	100	7·155	Kaolinite	100	7·166	Kaolinite
15	4·446	do	30	5·001	Muscovite	10	4·47	Muscovite	5	4·984	Muscovite	25	4·443	do
20	4·354	do	35	4·471	do	15	4·255	Quartz	12	4·471	do	100	4·266	Quartz
17	4·172	do	10	4·358	Kaolinite	40 5	3·576 3·945	Kaolinite Kaolinite Muscovite	25	4·258	Quartz	20	4·163	Kaolinite
14	4·130	do	5	4·256	Quartz	5	3·844	Kaolinite	15	4·163	Kaolinite	8	3·843	do
8	3·837	do	5	4·044	Muscovite	5	3·735	do	10	3·863	do	8	3·704	do
75	3·576	do	8	3·883	do	8	2·562	Kaolinite Muscovite	5	3·735	do	55	3·576	do
5	3·346	Quartz	10	3·735	do	10	2·491	Kaolinite	70	3·584	do	V.S.	3·343	Quartz
3	3·099	Kaolinite	25	3·670	Serpentine ?	10	2·461	Quartz	8	3·492	do	8	3·027	Talc
14	2·561	do	50	3·578	Kaolinite	10	2·377	Kaolinite	V.S.	3·445	Quartz	15	2·560	Kaolinite
8	2·527	do	60	3·343	Quartz Muscovite	10	2·279	Kaolinite Quartz	5	3·027	Kaolinite Talc	5	2·526	do
12	2·489	do	40	3·202	Muscovite	5	2·238	Quartz	5	2·985	Muscovite	8	2·495	Kaolinite Talc
8	2·379	do	5	3·064	Kaolinite	8	2·125	Quartz Kaolinite	10	2·562	Kaolinite Muscovite	25	2·458	Quartz
20	2·339	do	20	2·995	Kaolinite Muscovite	8	1·989	Muscovite Kaolinite	8	2·492	Kaolinite	8	2·376	Kaolinite

12	2·287	do	10	2·862	Muscovite	5	1·974	Quartz	10	2·458	Quartz	15	2·336	do
3	2·180	do	5	2·791	do	18	1·819	do	8	2·381	Kaolinite	20	2·281	Kaolinite Quartz
5	1·992	do	5	2·740	Kaolinite	10	1·665	Kaolinite	12	2·335	do	5	2·238	Quartz
5	1·983	do	15	2·564	Kaolinite Muscovite Serpentine	15	1·642	Muscovite	12	2·279	Quartz Kaolinite	15	2·132	do
3	1·938	do	10	2·495	Kaolinite	5	1·451	Quartz	5	2·238	Quartz	15	1·981	do
3	1·834	do	5	2·390	do	5	1·381	do	8	2·129	Quartz Muscovite	50	1·819	do
3	1·786	do	5	2·340	do	8	1·375	do	10	1·972	Quartz	15	1·674	do
6	1·659	do	5	2·296	do	8	1·371	do	20	1·819	do	12	1·661	Quartz Kaolinite
3	1·616	do	5	2·246	do	5	1·337	Muscovite Sericite ?	10	1·672	do	25	1·542	Quartz
2	1·541	do	5	2·204	do	5	1·287	Muscovite	10	1·667	Kaolinite	8	1·487	Kaolinite
12	1·489	do	5	2·127	do	5	1·255	Quartz	10	1·542	Quartz	5	1·453	Quartz
2	1·456	do	15	1·993	Muscovite				8	1·492	Kaolinite	12	1·382	do
2	1·371	do	5	1·658	Kaolinite				8	1·382	Quartz	12	1·377	Quartz Talc
2	1·307	do	5	1·503	Muscovite				10	1·377	Quartz Talc Muscovite	15	1·373	Quartz
			5	1·351	do				8	1·371	Quartz Kaolinite	5	1·258	do
									5	1·255	Quartz	5	1·183	do

1. Supplied by Ceramic Expert, Kundra.
2. Supplied by Baidyanath Sarda, Chaibasa.
3. Supplied by Orissa Industries Ltd.
4. Supplied by Perfect Potteries Ltd.
5. Supplied by Reliance Firebrick and Pottery Co., Ltd.

reproduced in Fig. 3. These patterns were recorded for reproduction purposes with the recorder chart moving at the rate of 9″ per hour. These records show a slightly more irregular background than the originals, from which the *d*-values were calculated, which were recorded at 36″ per hour.

The differential thermal curves of these clays are given in Fig. 2. All these clays show broad endothermic peaks between 586–610° C. and a comparatively sharp exothermic peak between 975 and 990° C., characteristic of kaolinite. The endothermic peak is thought to be due to the loss of combined water and the exothermic peak due to the crystallisation of alpha alumina or mullite, or both.[4] A small exothermic peak at 450° C. in the Rajhara clay appears to be due to the oxidation of some organic matter. During

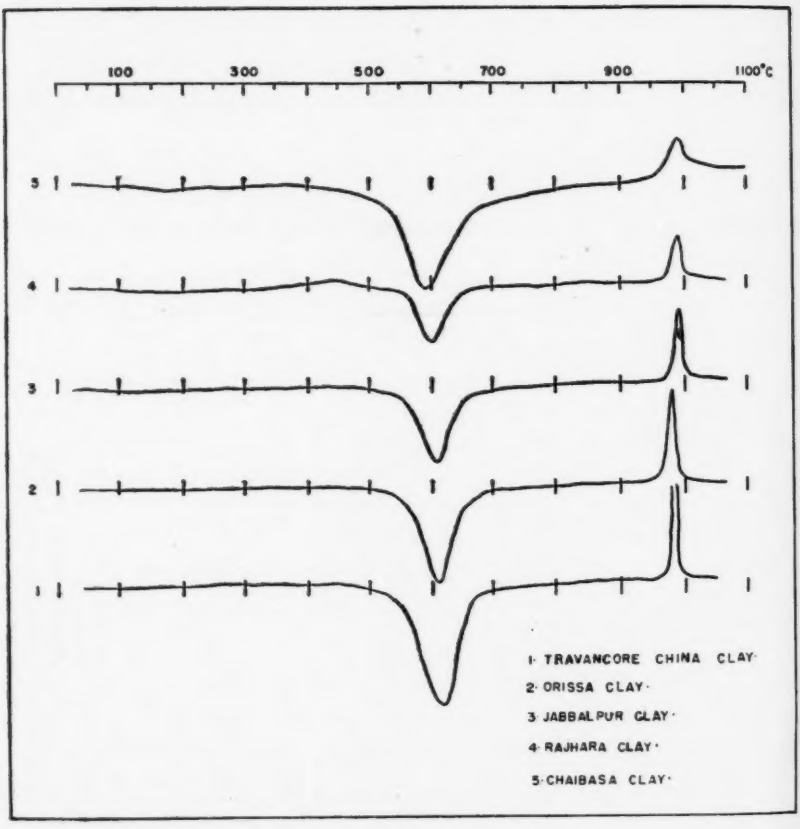

FIG. 2. Differential Thermal Curves.

cooling all the clays showed a small exothermic peak at 573° C. which is attributed to the β to α inversion of quartz.

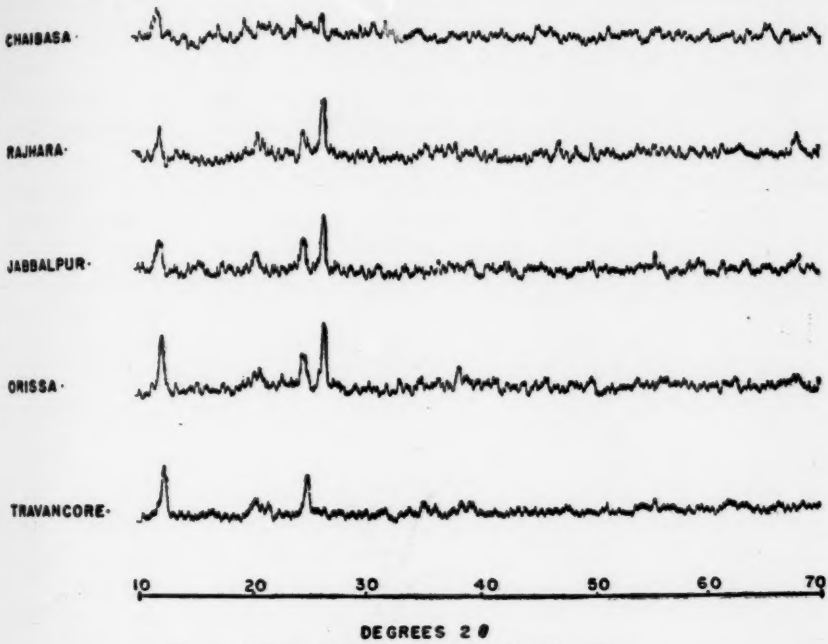

FIG. 3. X-Ray Diffraction Patterns of Indian Clays.

The electron micrographs of these clays are shown in Figs. 4–8. The Travancore-China clay is extremely well crystallised, and shows equant or elongated crystals of six-sided cross-section. The Jabbalpur clay also shows many such well-formed crystals besides the coarsely formed irregular plates. The Orissa clay shows a few subhedral crystals with the irregularly formed plates predominating. The Rajhara clay is mostly composed of irregularly formed coarse plates with some smaller subhedral to anhedral crystals. The shape of the crystals in all these clays is suggestive of kaolinite with a possibility of the coarser plates being dickite. A recent publication[5] shows that kaolinite could occur in tubular forms. However, such forms were not seen in the present study. The Chaibasa clay is very coarsely crystalline, showing large irregular plates. Some of these could possibly be mica.

Under the petrographic microscope the clay mineral, in most cases, appears as aggregates of minute plates and needles, with an average refractive index of 1·562, and with moderate to weak birefringence. In the Chaibasa

clay, some of these small plates, under high magnification, appear to be vermicular. The impurities present in these clays are as follows:

Travancore-China clay	A small amount of quartz with traces of rutile, zircon, apatite, hydrated iron oxide and muscovite.
Chaibasa clay	Appreciable amounts of muscovite and kyanite, small amounts of serpentine and quartz, and a trace of hæmatite.
Orissa clay	Small amounts of quartz and muscovite, with traces of rutile, limonite, apatite, dolomite, zircon, sericite and orthoclase.
Jabbalpur clay	Small amounts of quartz and sericite (muscovite) and talc, with traces of rutile, apatite, calcite and gibbsite.
Rajhara clay	A considerable amount of quartz with a small amount of talc, traces of apatite, calcite, and hydrated iron oxides.

SUMMARY

The principal constituent in all these clays is kaolinite. It is fine-grained and very well crystallised in the Travancore-China clay. In Jabbalpur, Orissa and Rajhara clays, the kaolinite occurs mostly as coarse irregular plates with some fine euhedral to subhedral crystals. The Chaibasa clay shows the coarsest plates, some of which seem to be muscovite. Amongst the impurities, quartz occurs in all these clays in varying amounts, the Rajhara clay containing the largest amount. Muscovite occurs in a significant amount in the Chaibasa clay, and in small amounts in Orissa, Jabbalpur and Travancore-China clays. Kyanite occurs in an appreciable amount in Chaibasa clay, along with a small amount of serpentine. Small amounts of talc occur in the Rajhara and Jabbalpur clays. The Rajhara clay contains some organic matter. Other impurities occurring in very small amounts or traces are rutile, hæmatite, apatite, zircon, orthoclase, calcite, dolomite, gibbsite and hydrated iron oxides.

ACKNOWLEDGEMENTS

I take this opportunity to thank Dr. F. W. Boswell for his valuable help in the electron microscopic study. My thanks are due to Dr. A. T. Prince and Dr. N. F. H. Bright, for helpful suggestions during the course of the investigation and also during the preparation of this publication, and to Mr. R. H. Lake, for his help in conducting the differential thermal analyses.

FIG. 4. Travancore China Clay, × 20,000

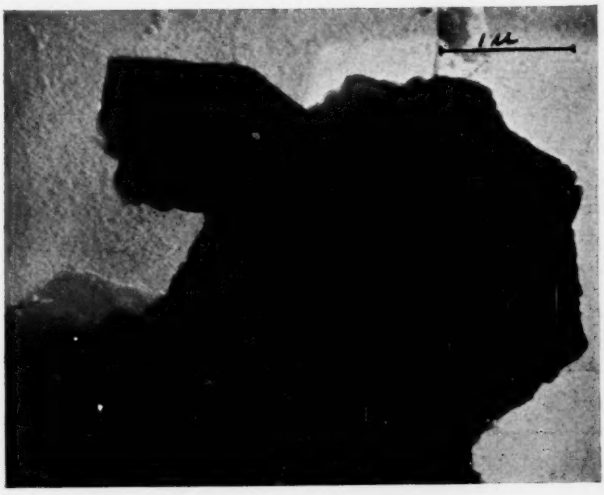

FIG. 5. Chaibasa Clay, × 20,000

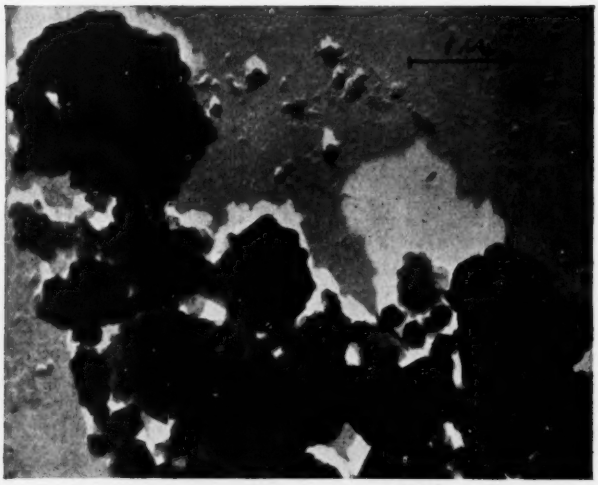

FIG. 6. Orissa Clay, × 20,000

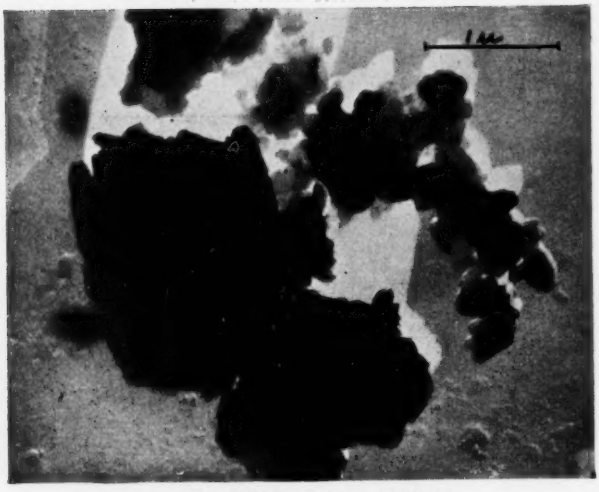

FIG. 7. Jabbalpur Clay. × 20,000

FIG. 8. Rajhara Clay. × 20,000

References

1. Grim, R. E. .. *Clay Mineralogy*, McGraw-Hill Book Co, Inc., New York, 1953.
2. Klug, H. P. and Alexander, L. E. *X-Ray Diffraction Procedures*, John Wiley & Sons, Inc., New York, 1954.
3. Kerr, P. F., Hamilton, P. K. and Pill, R. J. *et al.* *Analytical Data on Reference Clay Minerals*, American Petroleum Institute, Project 49, Preliminary Report No. 7, 1950.
4. Grim, R. E. .. *Clay Mineralogy*, McGraw-Hill Book Co., Inc., New York, 1953.
5. Stourdze, U. Y., Nicot, B. N. F. and Goulart de Andrade, E. "Tubular Morphology of Some Brazilian Kaolinites," *Am. Mineral.*, 1956, **41**, 67–75.

THE ROLE OF SOLVENT IN CHEMICAL REACTIONS

Part II.* The Reaction between Aniline and Methyl Iodide in Different Solvents

By V. S. Padmanabhan‡

(Contribution from the Chemistry Department, Madras Christian College, Tambaram)

Received March 19, 1956

(Communicated by Dr. S. V. Anantakrishnan, F.A.SC.)

In the previous part[1] were reported some observations on the influence of solvents on the reaction between pyridine and methyl iodide. The present studies deal with the alkylation of a primary amine. While the first reaction was comparatively simple, here there are two complications—consecutive reactions of progressive alkylation, replacing the hydrogen atom of the primary amine and then formation of the quaternary ammonium compound. While the two substitution reactions may involve comparable activation energies, the formation of the quaternary ammoium compound may involve a lower activation energy. Cox[2] has studied the reaction between aniline and ω-bromo acetophenone in several solvents while Hawkins[3] has studied the reaction between pyridine and allyl bromide in different solvents. Neither worker has been able to notice any specific correlation between any of the physical properties of the solvent and the reaction rate. The reactions had also been studied by these workers under conditions in which heterogeneity could not be excluded. Subsequent work also indicates the use of benzyl bromide[4] and allyl chloride[5] in the reaction with pyridine and it has been observed that the influence of dielectric constant is sometimes in opposite directions when the different halides are compared. It was felt that the use of methyl halides in the first instance will simplify the situation and serve as a starting point in the analysis of solvent influences.

The reaction between aniline and methyl iodide proceeded under homogeneous conditions in both acetone and ethyl alcohol but in nitrobenzene and carbon tetrachloride solutions even in very dilute solutions separation of a solid product was evident quite early in the course of the reaction. The

---

* Based on the Thesis approved for Ph.D. Degree of Madras University.

‡ Now at the Central Leather Research Institute, Madras-20.

analysis of both precipitate and solution from time to time for nitrogen as well as iodide contents showed clearly that the solid separating was primarily aniline hydriodide while the solution contained the products of progressive alkylation, depending on the duration of the reaction. The reaction apparently did not go to completion, the amount of methyl iodide used up being only about 87% at about 35° C. even after eight months.

Irrespective of the solvent used, the initial rate, whether one takes the value obtained by graphical extrapolation of experimental data or actual calculated value for the first 10% of the reaction, differed to varying extents, from the mean value of the rate constant. The reaction was found to be best considered as a second order one even though there was a pronounced drift in the value. For purpose of discussion, the values are collected together in Tables I, II, III and the drift in the values of the rate constants illustrated in Figs. 1 and 2 below:

TABLE I

The reaction in nitrobenzene

[Aniline] : [methyl iodide]	Temperature ° C.	Initial value of bimolecular rate constant $\times 10^4$	Mean value of bimolecular rate constant $\times 10^4$
1·50	50	2·33	2·80
1·53	60	4·29	4·69
1·15	40	1·62	1·73
1·26	50	2·29	2·63
0·85	45	1·62	1·88
0·74	50	2·31	2·72
0·89	50	2·45	2·71
0·87	55	3·46	3·74
0·87	60	5·39	5·02

TABLE II

The reaction in acetone

[Aniline]: [methyl iodide]	Temperature ° C.	Initial value of bimolecular rate constant $\times 10^4$	Mean value of bimolecular rate constant $\times 10^4$
1·44	40	2·70	3·11
1·28	50	5·74	6·03
0·79	40	1·87	1·64
0·88	40	2·37	2·41
0·88	45	3·30	3·35
0·91	50	4·81	4·50
0·86	50	4·22	4·57
0·87	55	6·11	6·18

TABLE III

Solvent	Temperature° C.	% Reaction	$k_2 \times 10^4$	$k_1 \times 10^4$
Nitrobenzene ..	40	8·49	1·618	1·478
		27·57	1·646	1·345
		43·03	1·706	1·236
		55·76	1·738	1·132
		63·95	1·793	1·063
95% Ethyl alcohol ..	60	28·39	16·82	
		48·12	17·55	
		62·10	17·51	
Acetone	50	13·11	4·81	
		29·38	4·75	
		39·62	4·55	
		47·37	4·49	
		57·10	4·35	

N.B.:—In all the tables, concentrations are approx. M/10, all rate constants in moles. litre and the unit of time is the second.

2. In Table III, k_1-First order rate const. calcd. with respect to methyl iodide.

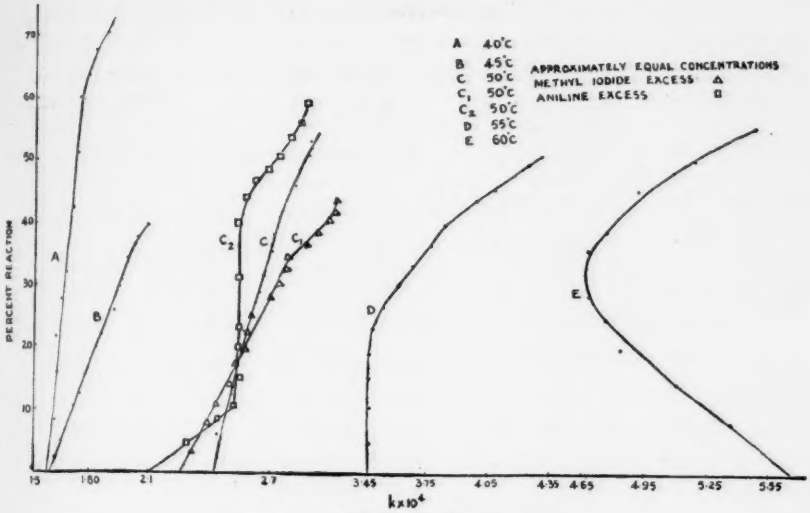

FIG. 1. Reaction in Nitrobenzene

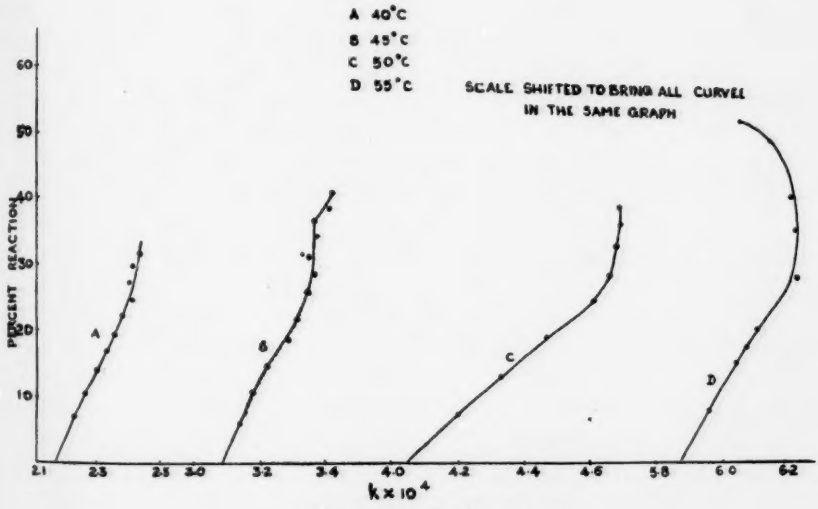

FIG. 2. Reaction in Acetone

Grant and Hinshelwood[6] in their study of benzoylation of aniline found that the best constants were obtained when the proportion of amine to acyl

halide was 2 : 1, the second molecule of the amine serving to prevent the reversal of the reaction. If similar conditions were to hold good in the alkylation studied here, with the consumption of methyl iodide as the measured quantity, one might expect that the rate expression of the type:

$$dx/dt = k_2 (a - x) (b - 2x)$$

will apply but calculations showed that no constant could be obtained using the integrated form of this equation. The formation of aniline hydrochloride as well as the drift in the rate constant call for a different explanation.

The following stages can be visualised for the reaction:

$$C_6H_5NH_2 + MeI \longrightarrow (C_6H_5NH_2Me)^+ + I^- \qquad (i)$$

$$(C_6H_5NH_2Me)^+ \longrightarrow C_6H_5NHMe + H^+ \qquad (ii)$$

$$(C_6H_5NH_2Me)^+ \longrightarrow C_6H_5NH_2 + Me^+ \qquad (iii)$$

Ionisation of methyl iodide is unlikely to be first stage in reaction since the rate is found to be quite dependent on the initial concentration. The first reaction is clearly the rate-determining step and the general trend of rate constants is that of a second order. (ii) and (iii) are reversible reactions and in the presence of an adequate quantity of aniline, reaction (*iii*) will be negligible. The reversibility could be readily demonstrated by starting with an alkyl aniline hydrochloride. After contact with a solution of aniline in the different solvents, the final product analysed to indicate the interchange, the solid being essentially aniline hydrochloride.

TABLE IV

Solvent	Dielectric constant at 20° C.	Bimolecular rate constants × 10^4					Arrhenius parameters	
		40° C.	45° C.	50° C.	55° C.	60° C.	E K. Cals.	$\log_{10}PZ$
Acetone ..	31·0	2·17	3·09	4·06	5·88	..	13·23	5·59
Ethyl alcohol (95%) ..	40	4·07	..	8·86	..	17·7	15·37	7·35
Nitrobenzene	35·79	..	1·60	2·44	3·46	5·67	16·83	7·80

N.B.—The rate constants in acetone and nitrobenzene have been obtained from experiments in which the ratio Aniline: Methyl iodide was in the region 0·85–0·90.

Since the reaction appeared to be sensitive to even small changes in the concentrations, the order of the reaction could be computed only by van't

Hoff's differential method and these indicate that the reaction is of the first order with reference to aniline but the reaction order with respect to methyl iodide is only half. Since the measured quantity is only the change in methyl iodide concentrations and part of the iodide is fixed as aniline hydriodide, further work is needed to indicate the path of the reaction in full. With this limitation, however, we can analyse the influence of the solvent.

For reasons already indicated, comparison could be made using the initial value of the bimolecular rate constant (obtained by extrapolating k_2% reaction graph to 0% reaction), in the different solvents at different temperatures. Some justification for this procedure is the observation that the log $k - 1/T$ graph showed very good linear relationship (Fig. 3).

It is clear that while there is a corresponding change in both Arrhenius' parameters similar to that indicated by Fairclough and Hinshelwood,[7] there does not appear to be any correlation with dielectric constant, of the type expected for a dipole-dipole reaction. Solvation of the transition state, removal of the proton as a solvated ion in the second stage of the reaction, changes in the dielectric constant with temperature (which have not been taken note of in the present calculations), solubility of the different products —all are relevant factors to be taken into account and further information is clearly needed. As a first step, solvent mixtures might be expected to give useful data and these are considered in the next part. The complex nature of specific solvent influences are shown clearly by the rate constant, the reaction being fastest with 95% ethyl alcohol even though the activation energy in this solvent is much higher than in acetone.

If the solvent is to take part in proton removal, the alternative question arises: Is there any unimolecular change with ionisation of methyl iodide as the rate determining step ? This step cannot be ruled out on account of the high dielectric constant of the media. Hughes, Ingold and Shapiro[8] have shown, for instance, that where, as in the case of Isopropyl halides, both S_N1 and S_N2 mechanisms are possible, the rate constant may show a continuous rise. This feature is present in the present reaction at the lower temperatures but at the highest temperatures studied and probably at the later stage in the reaction the trend is reversed and there is a sign of decrease. At the present stage, it is not possible to isolate the two types of reaction and with a primary amine further alkylations which also consume the alkyl halides, are unavoidable so that the consumption of methyl iodide appears to be more than can be accounted for by the first stage of the alkylation. In either case, it is clear that the introduction of an alkyl group is analogous to the formation of ' Onium compounds '.

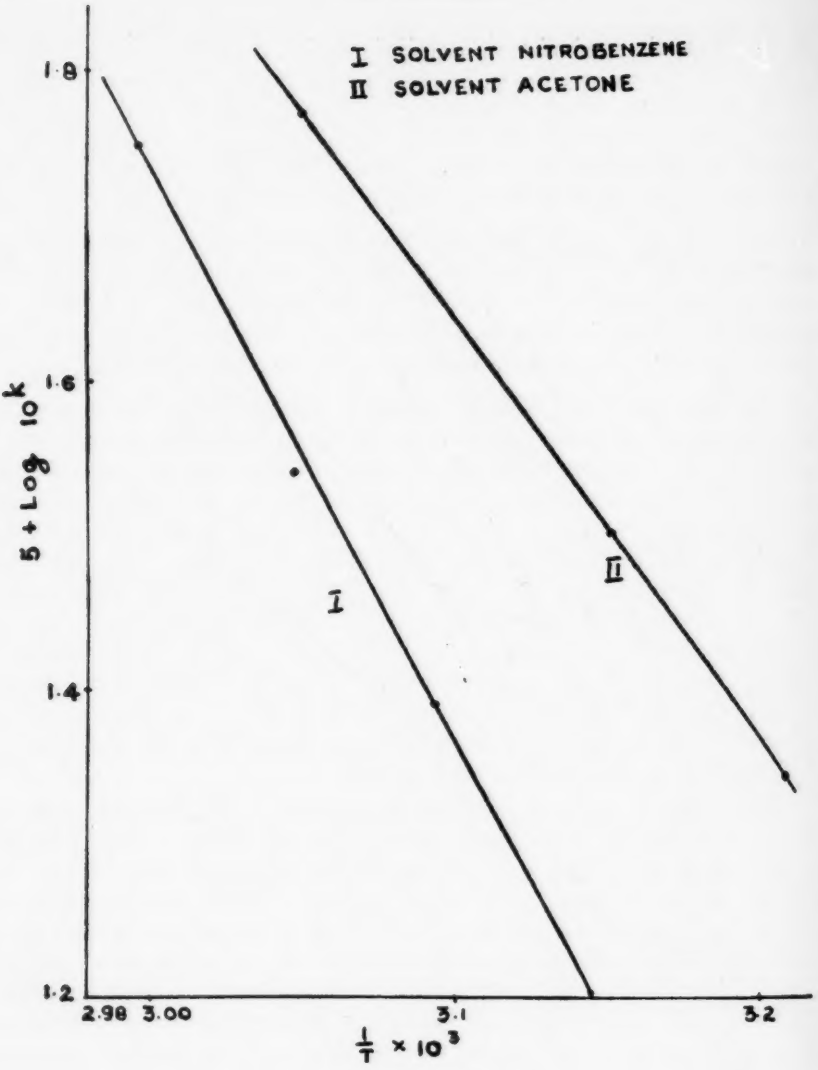

FIG. 3

EXPERIMENTAL

Aniline, redistilled, B.D.H., was distilled once, kept over Analar potassium hydroxide for a week and then redistilled with the minimum exposure to light. Even diffuse daylight was found to cause the deepening in the colour

of the distillate. Rejecting large head and tail fractions, only the middle fraction was collected, B.P. 183° C./760 mm.

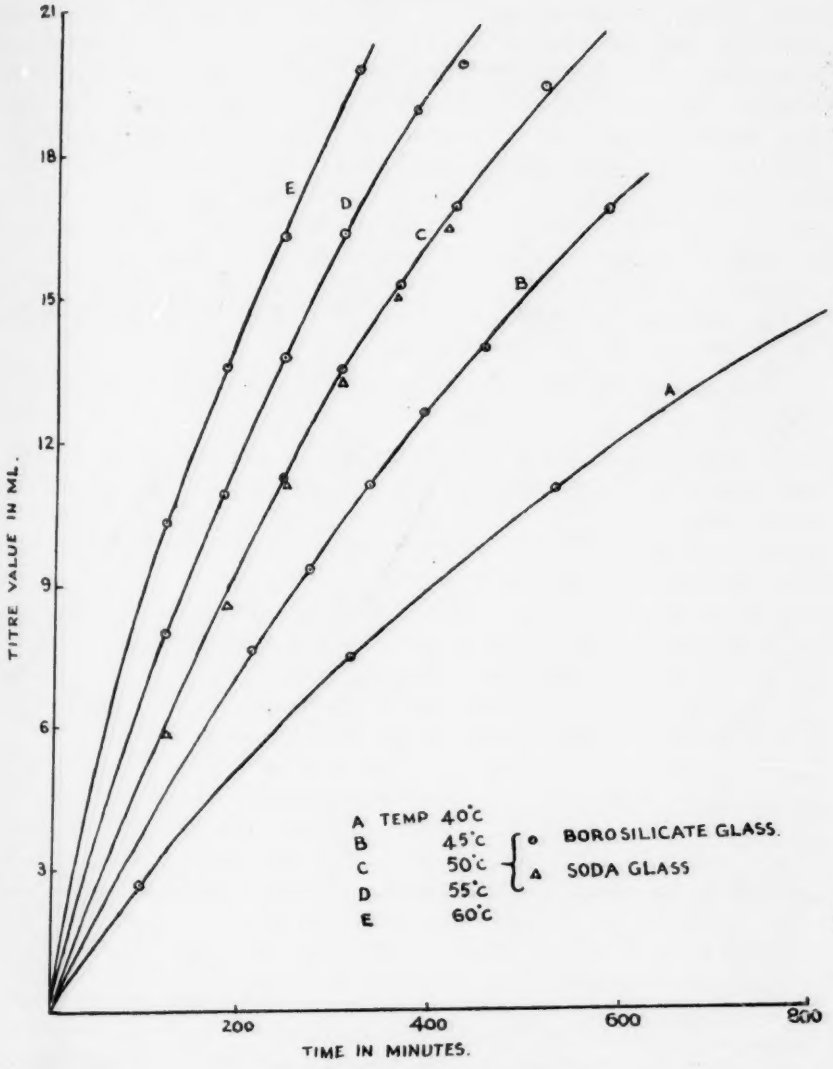

FIG. 4, Solvent : Nitrobenzene

Methyl iodide was purified as in the previous part.[1]

Nitrobenzene, pure redistilled, B.D.H., was shaken repeatedly with small portions of sodium carbonate solution till the aqueous portion was colourless, then washed repeatedly with distilled water, left over anhydrous calcium chloride in the dark for a week and then fractionated, only the middle fraction being used, B.P. 210° C./760 mm. Moelwyn-Hughes[9] considered that this drying agent was not adequate but it was found that by using long periods of drying and rejecting large head and tail fractions, contamination by moisture is negligible. The amine hydriodides formed in the reaction are found to be appreciably soluble even in the presence of minute amounts of water in the solvent and a test for the absence of water in the solvents is the ready precipitation of the salts even in the most dilute solutions. Further, it was observed that freshly distilled nitrobenzene is very pale in colour which deepens with the absorption of moisture.

Acetone of Laboratory Reagent quality was purified as in the previous part.[1]

Carbon tetrachloride of redistilled grade was left over mercury, shaken at frequent intervals until there was no further formation of mercuric sulphide, then washed thoroughly with sodium bicarbonate and then with distilled water, and finally dried over anhydrous calcium chloride and fractionated B.P. 75·6° C./760 mm.

Preliminary experiments.—Aniline and methyl iodide reacted vigorously with considerable evolution of heat. In nitrobenzene, the reaction was still exothermic but much slower. Leafy white crystals with no sharp melting are generally obtained. Estimation of the iodide content gave a value nearer to aniline hydriodide than to the alkylated product. (In the course of these studies, it has been found that estimations using Fajans' method with eosin as the indicator gave more consistent results.) The results show clearly that the product separating out was essentially aniline hydriodide with about 3% of methyl aniline hydriodide. Nitrogen estimations by microkjeldahl methods gave identical results. Relative proportions did not alter the nature of the precipitated product. The examination of the mother liquor indicated the presence of alkylated products at all stages of methylation. The reaction in carbon tetrachloride was slower and the precipitate obtained had as before no sharp melting point. Estimation of iodide content indicated that invariably it was of mixed composition. Similar results were obtained using chloroform and acetic acid as solvents, the reaction being extremely slow in the last named solvent.

Typical results of analyses are presented in Table V.

TABLE V

	Nitrobenzene solutions			Carbon tetrachloride solutions	
	Precipitate		Mother liquor		
Experiment No.	4	5	45	11	50 (Left over for 8 months)
Concentration of aniline ..	M/10	M/5	M/5	M/10	M/5
Concentration of methyl iodide	M/10	M/10	M/5	M/10	M/5
Per cent. nitrogen ..	6·352	6·305		..	..
Per cent. iodine ..	57·35		48·67	56·15	56·08 & 56·74

Aniline hydriodide requires nitrogen 6·339% and iodine 57·46%.

Kinetic studies.—The reactions were studied in a large thermostat, electrically operated and maintained at the requisite temperature with a tolerance of $\pm 0{\cdot}005$ at 40°, $\pm 0{\cdot}01$ at 50° and $\pm 0{\cdot}015$ at 60° C. The reactant solutions were prepared by weighing both solvent and solute and thoroughly mixing the two in well-stoppered bottles. Measured equal volumes of these were pipetted into bulbs of borosilicate glass and sealed. A number of these sealed tubes were kept in the thermostat, and from time to time taken out and analysed.

The contents of the bulb were transferred to a separating funnel, rinsing the bulb with ice-cold distilled water, shaken with benzene sufficient to form an upper layer dissolving the reaction mixture. The aqueous layer was tapped off and the benzene layer extracted four times with ice-cold water. All the aqueous portions were combined and the iodide content estimated by Fajans' method using eosin as indicator.

Where the solvent was miscible with water, the contents of the bulb were taken up with ice-cold water to which sufficient acetic acid was added to chill the reaction and the iodide estimated with silver nitrate solution.

Typical runs in the different solvents are presented in Tables VI to IX.

TABLE VI

Reaction in nitrobenzene

Temperature	40° C.		50° C.		60° C.	
Aniline concentration	0·09434 mol./l.		0·03466 mol./l.		0·1074 mol./l.	
Methyl iodide concentration ..	0·08414 „		0·01839 „		0·07004 „	
Strength of $AgNO_3$ solution ..	0·0255 N		0·01048 N		0·02462 N	
	Time	V	Time	V	Time	V
	5880	2·75	19780	2·50	3600	4·15
	18876	7·55	43890	5·50	7200	7·95
	31600	11·15	49855	6·10	10800	10·45
	74830	18·85	59800	7·25	14400	12·65
	103500	21·85	77650	8·75	18000	14·98
	132400	24·20	95940	9·93	21600	16·75

TABLE VII

Reaction at 50° C. in nitrobenzene for elucidating reaction order

Concentration of aniline	0·09674 mol./l.	0·09674 mol./l.	0·09731 mol./l.	0·1390 mol./l.
Concentration of methyl iodide	0·09491 mol./l.	0·13060 mol./l.	0·1098 mol./l.	0·1098 mol./l.
Strength of $AgNO_3$ solution	0·02514 N in all the four experiments			

Time	V	Time	V	Time	V	Time	V
9000	6·85	9300	9·10	14400	11·25	10800	12·40
12600	8·95	12600	12·10	18300	13·60	14400	15·40
16200	10·75	16200	14·40	21600	15·30	18000	17·95
19800	12·60	19800	16·95	25200	17·00	21600	20·25
23400	14·35	23400	19·25	30600	19·50	25200	22·45
27000	16·20	27000	20·28	34200	20·00	28800	24·60
30600	17·05	30600	22·55	43200	23·25	32400	25·55

TABLE VIII

Reaction in 95% ethyl alcohol

Temperature °C.	40		50		60	
Concentration of aniline	0·09408 mol./l.		0·08732 mol./l.		0·1075 mol./l.	
Concentration of methyl iodide	0·08553 „		0·08839 „		0·08543 „	
Strength of $AgNO_3$ solution	0·02550 N.		0·02504 N		0·02462 N.	
	Time	V	Time	V	Time	V
	7725	7·90	7200	12·70	2100	9·85
	14890	12·60	10800	16·15	4500	16·70
	22270	16·10	14400	18·75	7500	21·55
	29540	18·60	18000	20·65	9300	23·65
	36850	20·30	21600	22·18	11700	25·75
	44080	21·6			14100	27·08
	62090	24·3			16500	24·40

TABLE IX

Reaction in acetone

Temperature °C.	40		50	
Concentration of aniline ..	0·08935 mol./l.		0·08650 mol./l.	
Concentration of methyl iodide	0·08946 „		0·08688 „	
Strength of $AgNO_3$ solution ..	0·02550 N.		0·02496 N.	
	Time	V	Time	V
	9218	5·55	7825	9·30
	16460	9·30	14400	13·05
	23570	11·85	25200	17·35
	32700	14·25	39600	20·90
	47130	17·35	61200	23·60
	76320	21·25		

Time in Seconds; V, Titre value in ml.

Examples of the general trend with other concentrations are illustrated in Figs. 5 and 6.

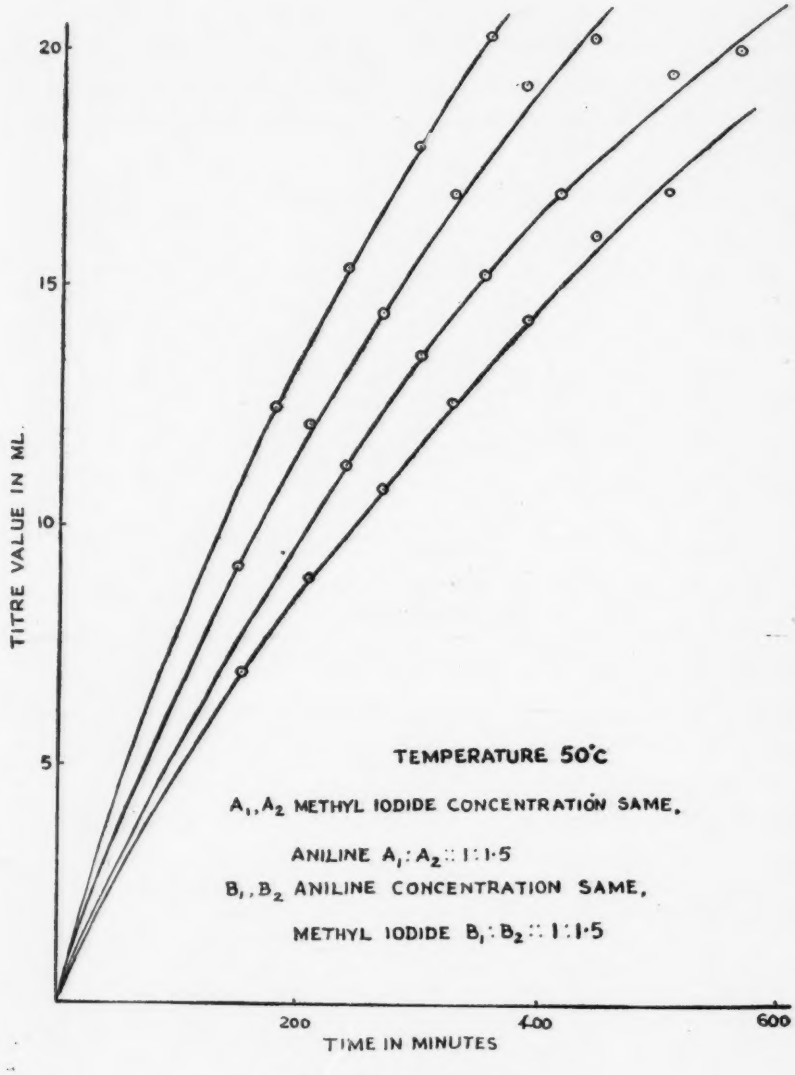

FIG. 5. Solvent Nitrobenzene

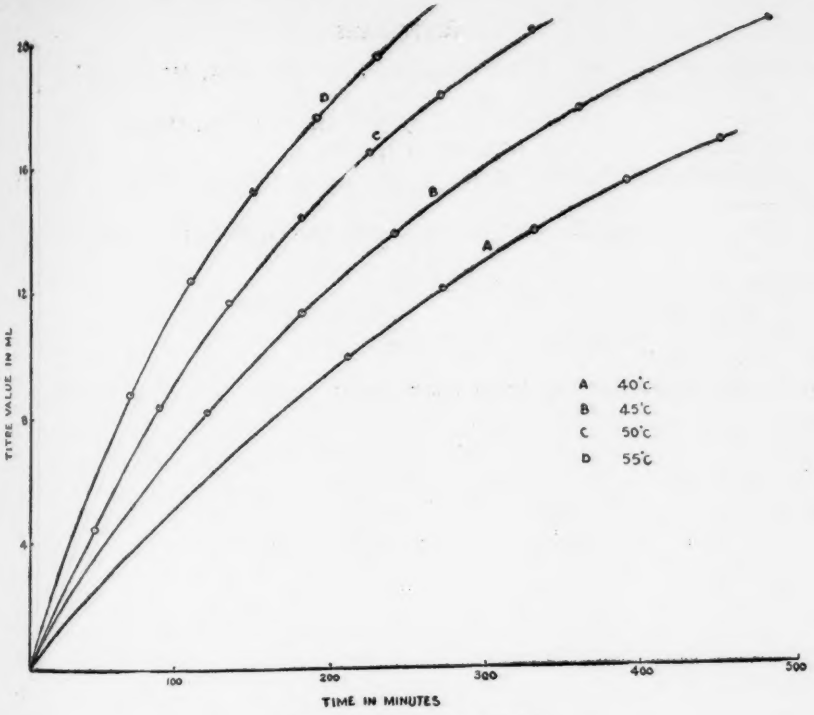

FIG. 6. Reaction in acetone

No kinetic studies were made in pure carbon tetrachloride as it was not possible even in the most dilute solutions to have homogeneous conditions. Similarly no kinetic studies were made in glacial acetic acid as the extent of reaction was small even after weeks.

SUMMARY

The reaction between aniline and methyl iodide has been studied at four different temperatures in 95% ethyl alcohol, acetone, nitrobenzene and carbon tetrachloride. The complications arising from progressive alkylations as well as from the crystallisation have been minimised under the experimental conditions in the initial stages. The observed changes in the rate constants and in the Arrhenius parameters are discussed.

ACKNOWLEDGEMENT

The author is deeply grateful to Prof. S. V. Anantakrishnan, M.A., Ph.D., F.R.I.C., F.A.Sc., for having suggested the problem and for his guidance and suggestions throughout the work.

REFERENCES

1. Padmanabhan, V. S. and Anantakrishnan, S. V. — *Proc. Indian Acad. Sci.*, 1954, **40 A**, 132.
2. Cox, H. E. .. *J. Chem. Soc.*, 1920, **117**, 493; 1921, **119**, 142.
3. Hawkins, J. A. .. *Ibid.*, 1922, **121**, 1170.
4. Moelwyn-Hughes, E. A. .. "Kinetics of Reactions in Solution," *O.U.P.*, 1947, 211.
5. ——— .. *Ibid.*
6. Grant, G. H. and Hinshelwood, C. N. — *J. Chem. Soc.*, 1933, 258; 1933, 1351.
7. Fairclough, F. A. and Hinshelwood, C. N. — *Ibid.*, 1937, 538.
8. Hughes, E. D., Ingold, C. K. and Shapiro, U. G. — *Ibid.*, 1936, 225.
9. Moelwyn-Hughes, E. A. .. Private communication.

POLAROGRAPHIC BEHAVIOUR OF METALS IN ETHANOLAMINES

Part II. Cadmium

By R. S. Subrahmanya

(*Department of General Chemistry, Indian Institute of Science, Bangalore-3*)

Received April 3, 1956

(Communicated by Prof. K. R. Krishnaswa ni, F.A.SC.)

Introduction

Jessop[1] has mentioned that cadmium gives rise to polarographic waves in presence of triethanolamine, but states that the top of the steps are rounded. Work conducted in this laboratory, however, has indicated that very good waves are obtained in presence of ethanolamines under certain conditions. In the present communication a detailed account is given of the polarographic behaviour of cadmium in presence of ethanolamines.

Experimental

The procedure employed in this work is essentially the same as that described previously.[2] The values of 'm' for the two dropping mercury electrodes used are 1·227 and 1·150 mg. per second respectively, the drop-time 't' being five seconds in normal potassium chloride. To facilitate comparison all the wave-heights recorded have been reduced to the corresponding values of the capillary with $m = 1·150$ mg. per second.

Results

1. *Effect of pH*

The results are summarised in Table I. In solutions containing mono- and diethanolamines at pH below 11, the polarographic wave seems to consist of two to three waves, the half-wave potentials of which are very close to each other. Beyond pH 11, these wavelets disappear and only one reversible wave appears. In triethanolamine solutions, between pH 9·8 and 6·5 two waves are noticed (Fig. 1). In more alkaline solutions, however, the second wave appears in the form of an elongated bend before the diffusion current plateau (Fig. 2). As the pH of the solution is increased, the half-wave potential increases slowly till a pH of about 9·8 is reached and thereafter it increases very rapidly. The value of $E_{3/4} - E_{1/4}$ varies between 0·031 and 0·049 V at different pH values indicating both reversible and irreversible electrode processes.

2. *Effect of variation of the composition of the base electrolyte*

The effect of addition of sodium hydroxide, sodium carbonate and ammonium chloride-ammonium hydroxide as the reagents to alter the pH has been investigated and the results obtained are indicated below. It may be pointed out that the half-wave potentials are not altered appreciably in solutions of pH less than 9.

TABLE I

Effect of pH on the Polarographic Behaviour of Cadmium in Ethanolamines

Amine used	pH	Half-wave potential *vs.* S.C.E. 1st wave (Volt)	$E_{3/4}-E_{1/4}$ 1st wave (Volt)	Half-wave potential *vs.* S.C.E. 2nd wave (Volt)	3rd wave (Volt)
Monoethanolamine ..	6·50	−0·57	..	−0·60	
	9·45	−0·63	..	−0·70	
	11·00	−0·65	..	−0·70	
	12·70	−0·73	..		
	13·50	−0·78	..		
Diethanolamine ..	6·05	−0·57	..	−0·61	−0·63
	9·45	−0·61	..	−0·64	−0·69
	10·70	−0·65	..	−0·70	−0·73
	12·70	−0·75	..		
	13·50	−0·80	..		
Triethanolamine ..	5·35	−0·597	0·031		
	6·50	−0·609	0·031	−0·80	
	7·20	−0·613	0·033	−0·80	
	8·65	−0·634	0·039	−0·80	
	9·80	−0·645	0·043	−0·80	
	11·20	−0·720	0·040		
	12·70	−0·771	0·031		
	13·50	−0·870	0·049		

(i) *Sodium hydroxide.*—A study of the polarograms obtained under different conditions has shown that in solutions containing triethanolamine the elongated bend (Figs. 2 and 3) before the diffusion current plateau is more marked in solutions with low amine/sodium hydroxide ratio, while in solutions containing mono- and diethanolamines perfectly sharp bends occur. The analysis of the waves obtained under varying conditions are presented in Table II. The half-wave potentials and the $E_{3/4}-E_{1/4}$ values of the waves for the triethanolamine complex are reported after

applying correction for the bend and are hence only approximate. From Table II it is clear that at a constant concentration of sodium hydroxide the half-wave potentials and $E_{3/4}-E_{1/4}$ values increase with an increase in the concentration of triethanolamine. It should be noted that the value of $E_{3/4}-E_{1/4}$ is about 0·035 V. at low concentrations of triethanolamine corresponding practically to a reversible 2-electron reduction step. In the

TABLE II

Effect of Sodium Hydroxide on the Polarographic Behaviour of Cadmium in Ethanolamines

Amine used	Concentration of		Half-wave potential *vs.* S.C.E. (Volt)	$E_{3/4}-E_{1/4}$ (Volt)	Height of the wave S/30	Concentration of cadmium (Millimolar)
	Amine (Molar)	Sodium hydroxide (Molar)				
Monoethanolamine	0·30	0·10	−0·753	0·027	slight pptn.	
	0·65	0·10	−0·777	0·032	,,	
	1·00	0·10	−0·794	0·029	47·5	1·089
	0·30	1·00	−0·815	0·025	slight pptn.	
	0·65	1·00	−0·836	0·032	,,	
	1·00	1·00	−0·849	0·032	44·0	
Diethanolamine	0·30	0·10	−0·750	0·028	slight pptn.	
	0·65	0·10	−0·773	0·029	45·7	
	1·00	0·10	−0·787	0·027	43·6	
	0·30	1·00	−0·324	0·030	42·2	1·089
	0·65	1·00	−0·846	0·033	41·8	
	1·00	1·00	−0·857	0·030	38·8	
Triethanolamine	0·02	0·10	−0·747	0·042	..	
	0·10	0·10	−0·771	0·031	49·1	1·068
	0·30	0·10	−0·825	0·051	46·2	1·122
	0·50	0·10	−0·857	0·124	43·8	1·122
	0·70	0·10	−0·885	0·099	41·3	1·122
			(Small bend)			
	1·00	0·10	−0·936	0·114	37·0	1·068
			(Bend has almost disappeared)			
	0·02	0·50	−0·837	0·036	..	
	0·10	0·50	−0·859	0·047	48·4	1·068
			(Slight elongated bend)			
	1·00	0·50	−1·010	0·102	35·2	1·068
	0·02	1·00	−0·860	0·036	..	
	0·10	1·00	−0·870	0·049	46·2	1·068
	0·30	1·00	−0·929	0·087	43·3	1·122
	0·50	1·00	−0·976	0·099	40·2	1·122
	0·70	1·00	−0·995	0·102	37·8	1·122
	1·00	1·00	−1·036	0·093	31·0	1·068

case of solutions containing mono- and diethanolamines, the half-wave potentials increase with the increase in the concentration of the amine while the value of $E_{3/4} - E_{1/4}$ is of the order of 0·028 V. under all conditions indicating a reversible 2-electron process. The wave-heights given in Table II indicate a decrease in the wave-height with an increase in the number of ethanol groups in the amine.

(ii) *Sodium carbonate.*—The results presented in Table III below indicate that the general behaviour in presence of sodium carbonate is the same as in the case of sodium hydroxide.

TABLE III

Effect of Sodium Carbonate on the Polarographic Behaviour of Cadmium in Ethanolamines

Concentration of cadmium = 1·089 millimolar

Amine used	Concentration of		Half-wave potential *vs.* S.C.E. (Volt)	$E_{3/4}-E_{1/4}$ (Volt)	Height of the wave
	Amine (Molar)	Sodium carbonate (Molar)			
Monoethanolamine	0·30	0·10	−0·739	0·029	52·0
	0·65	0·10	−0·764	0·032	51·4
	1·00	0·10	−0·772	0·032	51·3
	0·30	1·00	−0·767	0·029	42·4
	0·65	1·00	−0·787	0·029	40·8
	1·00	1·00	−0·797	0·023	39·3
Diethanolamine	0·30	0·10	−0·710	0·028	30·8 (Slight pptn.)
	0·65	0·10	−0·731	0·033	45·6
	1·00	0·10	−0·738	0·031	42·6
	0·30	1·00	−0·746	0·030	40·3
	0·65	1·00	−0·759	0·030	36·6
	1·00	1·00	−0·770	0·031	32·7
Triethanolamine	0·10	0·10	−0·707	0·037	38·1 (Slight precipitation)
	0·30	0·10	−0·739	0·056	44·7
	0·60	0·10	−0·767 / −0·915	0·053 / 0·109	41·3
	1·00	0·10	−0·806 / −0·951	0·062 / 0·100	37·6
	0·10	1·00	−0·759	0·055	45·2
	0·30	1·00	−0·789	0·058	35·3
	0·60	1·00	−0·822	0·063	31·9
	1·00	1·00	−0·859	0·800	28·6

(iii) *Ammonium chloride* (1 M)—*Ammonium hydroxide* (1 M).—The waves are very well defined. The half-wave potentials, the values of $E_{3/4} - E_{1/4}$, and the heights of the waves are given in Table IV. It is clear that the half-wave potentials increase with an increase in the concentration of the amine. The value of $E_{3/4} - E_{1/4}$ increases with an increase in the concentration of triethanolamine but in the case of mono- and diethanolamines the values are round about 0·029 V. indicating a reversible two-electron reduction process. The height of the wave diminishes very rapidly with increasing concentration of triethanolamine whereas in the case of mono- and diethanolamines the fall is not so great.

TABLE IV

Effect of Ammonium Chloride–Ammonium Hydroxide on the Polarographic Behaviour of Cadmium in Ethanolamines

Amine used	Concentration of amine (Molar)	Half-wave potential *vs.* S.C.E. (Volt)	$E_{3/4}-E_{1/4}$ (Volt)	Height of the wave at S/30	Concentration of cadmium (Millimolar)
Monoethanolamine	0·02	−0·784	0·027	67·5	1·089
	0·10	−0·791	0·030	66·7	
	1·00	−0·815	0·028	58·4	
Diethanolamine ..	0·02	−0·794	0·029	66·9	1·089
	0·10	−0·795	0·029	65·7	
	1·00	−0·807	0·026	54·9	
Triethanolamine ..	0·02	−0·757	0·029	63·4	1·034
	0·10	−0·762	0·033	62·1	
	0·30	−0·772	0·043	57·5	
	0·60	−0·786	0·041	48·4	
	1·00	−0·798	0·041	45·4	

3. *Effect of concentration of cadmium on the diffusion current constant in presence of sodium hydroxide, sodium carbonate and ammonium chloride* (1 *M*)*–ammonium hydroxide* (1 *M*).

The results obtained are presented in Table V. In solutions containing sodium hydroxide or carbonate, 0·5 or 1·0 M amine is employed due to low solubility of the complex. It has been noticed that the solubility of the monoethanolamine complex in sodium carbonate is greater than in sodium hydroxide solutions in contrast to the behaviour of the diethanolamine

TABLE V

*Effect of Concentration of Cadmium on the Diffusion Current Constant**

Conc. of cadmium (Millimolar)	Diffusion current constant $\frac{i_d}{Cm^{2/3}t^{1/6}}$	Concn. of cadmium (Millimolar)	Diffusion current constant $\frac{i_d}{Cm^{2/3}t^{1/6}}$
(1) *B.S.*: 1·00 *M Dien*+1·00 *M NaOH* $X = 1·436$ *at* $-1·0$ *V.*		(7) *B.S.*: 1·00 *M Trien*+1·00 *M* Na_2CO_3 $X = 1·426$ *at* $-1·1$ *V.*	
1·089	2·32	1·089	1·74
4·356	2·32	5·445	1·74
(2) *B.S.*: 0·50 *M Trien*+0·10 *M NaOH* $X = 1·417$ *at* $-1·3$ *V.*		(8) *B.S.*: 0·10 *M Moen*+*Ammonium chloride* (1*M*)+*Ammonium hydroxide* (1 *M*) $X = 1·447$ *at* $-1·0$ *V.*	
1·089	2·51	1·089	3·96
5·445	2·49	5·445	3·94
(3) *B.S.*: 0·50 *M Trien*+1·00 *M NaOH* $X = 1·417$ *at* $-1·3$ *V.*		(9) *B.S.*: 0·10 *M Dien*+*Ammonium chloride* (1 *M*)+*Ammonium hydroxide* (1 *M*) $X = 1·447$ *at* $-1·0$ *V.*	
1·089	2·31	1·089	3·90
5·445	2·28	5·445	3·88
(4) *B.S.*: 1·00 *M Moen*+1·00 *M* Na_2CO_3 $X = 1·435$ at $-1·0$ *V.*		(10) *B.S.*: 0·02 *M Trien*+*Ammonium chloride* (1 *M*)+*Ammonium hydroxide* (1 *M*) $X = 1·447$ *at* $-1·0$ *V.*	
1·089	2·35	1·034	3·96
5·445	2·33	5·170	3·93
10·89	2·32	(11) *B.S.*: 0·60 *M Trien*+*Ammonium chloride* (1 *M*)+*Ammonium hydroxide* (1*M*) $X = 1·431$ *at* $-1·0$ *V.*	
(5) *B.S.*: 1·00 *M Moen*+0·10 *M* Na_2CO_3 $X = 1·443$ *at* $-1·0$ *V.*		1·034	3·05
1·089	3·05	5·170	3·03
10·89	2·71		
(6) *B.S.*: 1·00 *M Trien*+0·10 *M* Na_2CO_3 $X = 1·426$ *at* $-1·1$ *V.*			
1·089	2·29		
5·445	2·24		

* *Abbreviations:*—B.S.–Base solution ; X–$m^{2/3}t^{1/6}$ in mg.$^{2/3}$sec.$^{-1/2}$; Moen–monoethanolamine ; Dien–diethanolamine ; Trien–triethanolamine.

complex whose solubility is greater in sodium hydroxide solutions. Solubility of the monoethanolamine complex in sodium hydroxide and that of diethanolamine complex in sodium carbonate is far too low to be of practical value. The results indicate that there is good proportionality

between diffusion current and the concentration of cadmium. The constancy of the diffusion current constant in presence of ammonium chloride-ammonium hydroxide is quite good, indicating that the presence of ethanolamines has no adverse effect.

Discussion

1. *Splitting of the polarographic wave in triethanolamine*

In solutions containing 0·1 M triethanolamine, it has been noticed that a doublet first appears at a pH 6·5, the half-wave potentials of the first and the second waves being *ca* — 0·61 V. and *ca* — 0·80 V. *vs.* S.C.E. respectively. As the pH is increased, the half-wave potential of the first wave increases (Table I) while that of the second remains practically constant. The doublet almost disappears as the pH is increased beyond 9·8. These observations can be explained as follows:—The single wave that appears at pH 5·35 is that of aquo-cadmium ion. As the pH is increased to 9·8, the first wave practically corresponds to that of aquo-cadmium ion while the second wave appearing at abou t— 0·75 V. *vs.* S.C.E. is perhaps due to triethanolamine-cadmium complex. When the pH is increased beyond 9·8, the half-wave potential of the first wave increases rapidly and when it approaches a value of *ca* — 0·75 V. *vs.* S.C.E. only a single wave with very little overvoltage is obtained. The wave-splitting is not due to two reduction states as the reduction of cadmium at the dropping mercury electrode involves only the straight two-electron reduction step, but due to the reduction of two species of complex ions in sluggish equilibrium. Such results have also been noticed by Lingane[3] while studying the polarographic behaviour of iron in tartrate media between pH 6 and 8.

When the base solutions contain 0·1 M triethanolamine and sodium hydroxide (Table II) or carbonate (Table III) the reduction process is very nearly reversible. As the concentration of triethanolamine is increased, the bend before the diffusion current plateau becomes elongated (at the same time $E_{3/4} - E_{1/4}$ value increases) indicating the formation of another species (containing more of the triethanolamine) in sluggish equilibrium.

2. *Splitting of the polarographic wave in mono- and diethanolamines*

In contrast to the behaviour in triethanolamine, the splitting of the polarographic wave is practically absent in base solutions containing mono- and diethanolamines except below pH 11. Below pH 11 two or three poorly separated waves (Table I) are seen, the lowest wave corresponding to aquo-cadmium ion while the next two are due to the complexes containing (i) cadmium ion + amine, (ii) cadmium ion + amine + hydroxyl. The formation

of the last species starts at pH 9·45. When the pH is increased beyond 11, only one wave is obtained showing the formation of complex (ii).

3. *Relationship between the height of the polarographic wave and the number of ethanol groups present in the complex-forming amine*

It has been noticed (Tables II, III, IV) that the wave-height for a given concentration of cadmium is highest in the case of monoethanolamine and falls off with an increase in the number of ethanol groups in the complex-forming amine. This indicates that the diffusion coefficient diminishes with an increase in the number of ethanol groups in the amine.

4. *Complex formation in presence of sodium hydroxide*

In base solutions containing mono- and diethanolamine, cadmium gives a reversible two-electron reduction step. Applying Lingane's[2] equation to the data presented in Table II we get that the complexes have the formulæ $[Cd(Moen)_2(OH)_2]$, $[Cd(Moen)_3(OH)_2]$ and $[Cd(Dien)_2(OH)_2]$. In this connection it has to be pointed out that the shift in the half-wave potential for a given concentration range of the amine is always smaller in solutions containing higher concentrations of sodium hydroxide. This observation may be explained on the basis of the co-ordination taking place through the hydroxyl of the ethanolamine. When there is very high concentration of the hydroxyl group the half-wave potential will have been shifted to a sufficiently negative potential which diminishes the effect of co-ordination through the hydroxyl of the ethanolamine.

The behaviour in triethanolamine solutions is completely different from that in mono- and diethanolamines. The shift in the half-wave potential is more complicated due to the following reasons: (1) the degree of irreversibility increases with the concentration of the amine; (2) there is wave-splitting and (3) the half-wave potentials are almost constant when the solution has high concentrations of sodium hydroxide (1·0 M) and a low concentration of triethanolamine. But, Lingane's[2] equation can only be applied to the region where the wave is only slightly irreversible. Under these conditions, the number of hydroxyl groups calculated for the complex is 4 and that of triethanolamine is unity. The formula of the complex can be written as $[Cd(Trien)_1(OH)_4]^{--}$.

5. *Complex formation in presence of sodium carbonate*

In sodium carbonate solutions also, the cadmium complex with mono- and diethanolamine gives a reversible polarographic wave. The formulæ arrived at by applying Lingane's equation are $Cd(Moen)_2CO_3$ and $Cd(Dien)_2CO_3$.

When triethanolamine is used as the complexing agent, application of Lingane's equation becomes very difficult, due to the marked interference of the second species of the complex and also due to the increasing irreversibility of the electrode process, with an increase in the concentration of triethanolamine. In 1·0 M carbonate solutions, the interference from the second species is not very great. The co-ordination of one molecule of triethanolamine with cadmium is obtained by the application of equations for irreversible waves.[2]

6. *Complex formation in presence of ammonium chloride-ammonium hydroxide*

In presence of ammonium chloride-ammonium hydroxide, the reduction process proceeds reversibly with mono- and diethanolamine. The shift in the half-wave potential indicates that one monoethanolamine molecule has entered into the complex. In the case of diethanolamine the shift is too small to suggest the entry of even one molecule of diethanolamine. When triethanolamine is used as the complexing agent the polarographic wave is reversible only at lower concentrations of the amine. By applying equations for irreversible waves[2] over the concentration range 0·3 to 1·0 M of the amine we get that one molecule of the amine has entered into the complex.

7. *Thermodynamic data from polarographic measurements*

(i) Hydroxide complex in monoethanolamine—[Cd $(Moen)_2 (OH)_2$].

The shift in the half-wave potential of a simple metal ion due to complex formation is given by the following expression[4]:—

$$(E_{1/2})_{\text{complex ion}} - (E_{1/2})_{\text{simple ion}} = (0{\cdot}06014/n) \log K_d - p\,(0{\cdot}06014/n) \log C_x$$
$$= E_c - E_s - p\,(0{\cdot}06014/n) \log C_x \qquad (1)$$

where,

K_d = dissociation constant of the complex,

C_x = excess concentration of the complex forming substance,

E_c = standard potential of the reaction

$$MX_p^{(n-pb)+} + ne \rightleftharpoons M\,(s) + pX^{-b} \qquad (2)$$

E_s = standard potential of the reaction

$$M^{n+} + ne \rightleftharpoons M\,(s) \qquad (3)$$

p and n have the usual significance.

When the concentration of monoethanolamine and hydroxyl are each equal to one molar the equation (1) takes the form

$$(E_{1/2})_{\text{complex ion}} - (E_{1/2})_{\text{simple ion}} = (0{\cdot}06014/n) \log K_d = E_c - E_s \quad (4)$$

The values of K_d and E_c are calculated from the above equation using the data given in this paper. $(E_{1/2})_{\text{simple ion}}$ has been taken to be $-0{\cdot}589$ V. *vs.* S.C.E. after incorporating theoretical temperature coefficient corrections[5] to the value at 25° C.[6] The standard potential at 30° C. of the reduction reaction, $Cd^{++} + 2e = Cd$ has been taken to be $-0{\cdot}402$ V.[7] (*vs.* N.H.E.). The value of $\Delta F°$ is calculated from the value of K_d by the following relation

$$\Delta F° = -RT \ln K_d \quad (5)$$

$Cd(Moen)_2(OH)_2 \rightarrow Cd^{++} + 2OH^- + 2$ Moen

$K_d = 2{\cdot}244 \times 10^{-9}$; $\Delta F° = 12{\cdot}00$ Kilocals.

$Cd + 2$ Moen $+ 2\ OH^- \rightarrow Cd(Moen)_2(OH)_2 + 2e$;

Standard potential $= +0{\cdot}662$ V. (*vs.* N.H.E.).

(ii) Carbonate complex in monoethanolamine — $Cd(Moen)_2(CO_3)_1$.

$Cd(Moen)_2(CO_3)_1 \rightarrow Cd^{++} + CO_3^{--} + 2$ Moen;

$K_d = 1{\cdot}205 \times 10^{-7}$; $\Delta F° = 9{\cdot}606$ Kilocals.

$Cd + 2$ Moen $+ CO_3^{--} \rightarrow Cd(Moen)_2(CO_3)_1 + 2e$;

Standard potential $= +0{\cdot}610$ V. (*vs.* N.H.E.).

(iii) Hydroxide complex in diethanolamine — $Cd(Dien)_2(OH)_2$.

$Cd(Dien)_2(OH)_2 \rightarrow Cd^{++} + 2\ OH^- + 2$ Dien;

$K_d = 1{\cdot}225 \times 10^{-9}$; $\Delta F° = 12{\cdot}38$ Kilocals.

$Cd + 2$ Dien $+ 2\ OH^- \rightarrow Cd(Dien)_2(OH)_2 + 2e$;

Standard potential $= +0{\cdot}670$ V. (*vs.* N.H.E.).

(iv) Carbonate complex in diethanolamine — $Cd(Dien)_2(CO_3)_1$

$Cd(Dien)_2(CO_3)_1 \rightarrow Cd^{++} + CO_3^{--} + 2$ Dien

$K_d = 9{\cdot}55 \times 10^{-7}$; $\Delta F° = 8{\cdot}359$ Kilocals.

$Cd + 2$ Dien $+ CO_3^{--} \rightarrow Cd(Dien)_2(CO_3)_1 + 2e$;

Standard potential $= +0{\cdot}583$ V. (*vs.* N.H.E.).

In the case of triethanolamine it is not possible to calculate the value of the thermodynamical constants as the electrode process is mostly irreversible. The irreversibility is possibly due to the three hydroxyl groups present in triethanolamine which appears to be responsible for the activated nature of the reduction process.

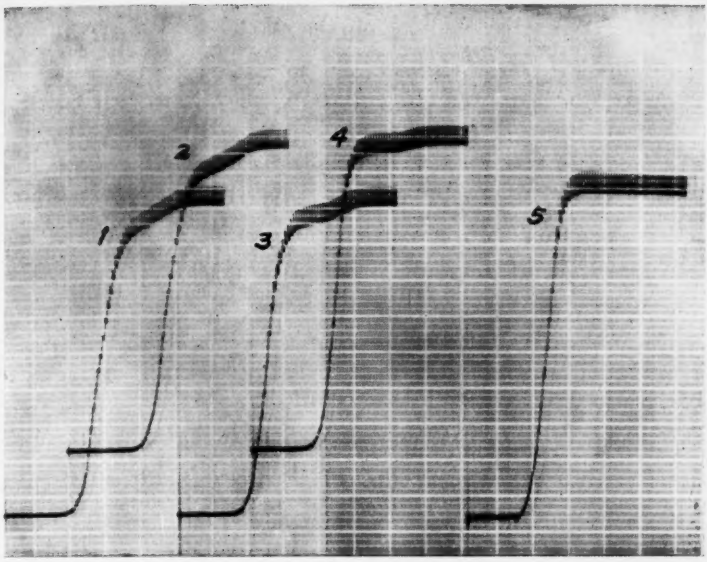

FIG. 1. Effect of pH on the polarographic behaviour of cadmium (1·068 millimolar) in presence of triethanolamine.

Curves 1 to 5 are taken at pH 9·80, 8·65, 7·20, 6·50 and 5·35 respectively. Sensitivity: S/30.

The voltage line just before the beginning of the polarogram corresponds to — 0·373 V. *vs.* S.C.E.

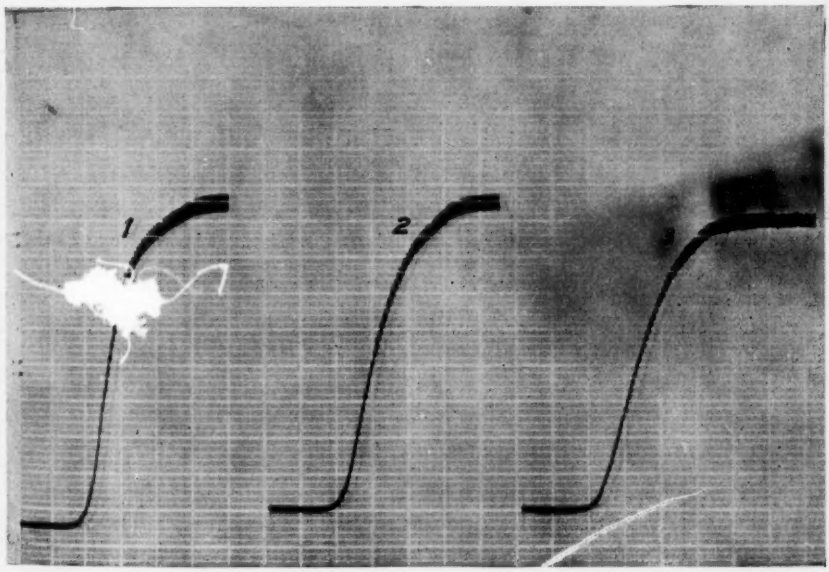

FIG. 2. Effect of sodium hydroxide on the polarographic behaviour of cadmium (1·122 millimolar) in presence of triethanolamine.

Curves 1, 2 and 3 have been taken in 0·1 M sodium hydroxide and 0·30, 0·50 and 0·70 M triethanolamine respectively. Sensitivity: S/30.

The voltage line just before the beginning of the polarogram corresponds to — 0·573 V. *vs.* S.C.E.

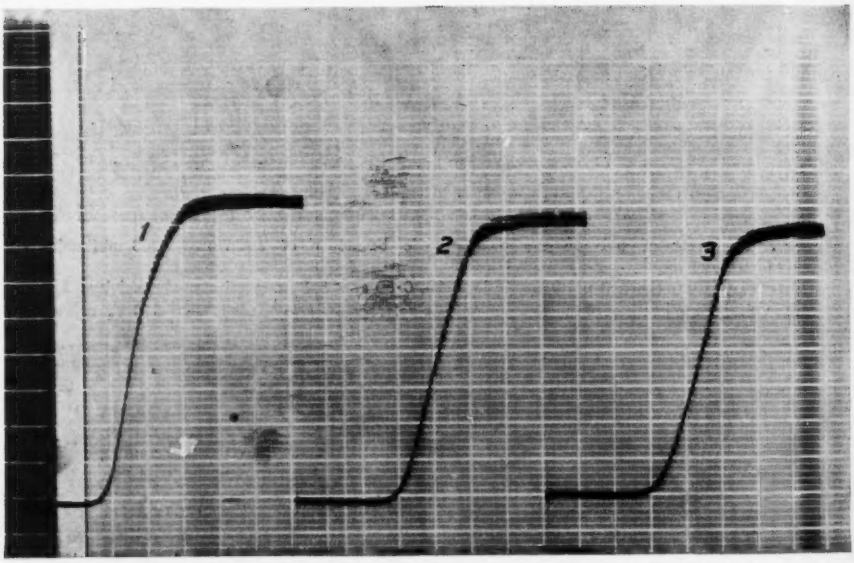

FIG. 3. Effect of sodium hydroxide (1·0 M) on the polarographic behaviour of cadmium (1·122 millimolar) in pre-ence of triethanolamine.

Curves 1, 2 and 3 are taken with 0·30, 0·50, and 0·70 M triethanolamine respectively. Sensitivity : S/30.

The voltage line just before the beginning of the polarogram corresponds to −0·573 V. *vs.* S.C.E.

Summary

1. A systematic study of the polarographic behaviour of cadmium has been carried out employing mono-, di- and triethanolamines as the complexing agents at various pH values and in presence of (i) sodium hydroxide, (ii) sodium carbonate and (iii) ammonium chloride-ammonium hydroxide.

2. In base solutions containing triethanolamine, there is a marked tendency for the splitting up of the polarographic wave, while this phenomenon is almost absent when mono- and diethanolamines are used as complexing agents except when pH is below 11.

3. The polarographic reduction is reversible in solutions containing mono- and diethanolamines and mostly irreversible in triethanolamine solutions. An explanation has been suggested for the irreversibility of the process in triethanolamine solutions.

4. The formation of the following complexes is indicated from polarographic data:—

$[Cd(Moen)_2(OH)_2]$ $[Cd(Moen)_3(OH)_2]$ $[Cd(Moen)_2(CO_3)_1]$

$[Cd(Moen)_1(NH_3)_x]^{++}$ $[Cd(Dien)_2(OH)_2]$ $[Cd(Dien)_2(CO_3)_1]$

$[Cd(Trien)_1(OH)_4]^{--}$ $[Cd(Trien)_1(NH_3)_y]^{++}$ $[Cd(Trien)_1(CO_3)_x]^{2-x}$.

5. Dissociation constant and the ΔF° value for the dissociation of the complex are calculated from polarographic measurements in the case of reversible reduction processes.

6. The use of mono- and diethanolamine in the base solutions is suitable for the polarographic estimation of cadmium.

Acknowledgement

The author wishes to express his sincere thanks to Prof. K. R. Krishnaswami and Dr. M. R. A. Rao for their kind interest and helpful discussions.

References

1. Jessop, G. .. *Nature.*, 1946, **158**, 59.
2. Subrahmanya, R. S. .. *Proc. Indian Acad. Sci.*, 1956, **43**, 133.
3. Lingane, J. J. .. *J. Amer. Chem. Soc.*, 1946, **68**, 2448.
4. Kolthoff, I. M. and Lingane, J. J. *Polarography*, 1952, **1**, 214–15, Interscience Publishers, New York.
5. ——— ——— .. *Ibid.*, p. 202.
6. ——— ——— .. *Ibid.*, p. 198.
7. Harned, H. S. and Fitzgerald, M. E. *J. Amer. Chem. Soc.*, 1936, **58**, 2624.

VARIATION WITH LUNAR PHASE OF MIDDAY CRITICAL FREQUENCIES AND HEIGHTS OF THE F2 LAYER OVER AHMEDABAD AND OTHER LOW LATITUDE STATIONS

By K. M. Kotadia and K. R. Ramanathan, F.A.Sc.

(*Physical Research Laboratory, Ahmedabad, India*)

Received May 15, 1956

Abstract

The paper contains an analysis of the variation of the midday values of foF_2, $h'F_2$ and hpF_2 with lunar phase at Ahmedabad during the years 1954 and 1955 and of foF_2 alone at Bombay, Madras and Tiruchirapalli during 1954. It is found that while the semidiurnal lunar tidal variations at Ahmedabad and Bombay agree in phase with those observed at middle latitudes, the phase reverses in direction between Bombay and Madras. The results are compared with those relating to Huancayo and Singapore.

Introduction

It is known that lunar tidal variations occur in the upper atmosphere as well as in the lower. The amplitudes of variation are much larger aloft and the phases are different. Martyn (1949) studied the F2 layer data of a number of places in middle latitudes and found that the variation was semidiurnal and that the amplitude of variation of foF2 (mean of all hours) range from 0·06 to 0·142 Mc/s and of hpF2 from 1·7 km to 3·6 km. The maximum phases of foF2 and hpF2 were found to be at 10 and 06 lunar hours. Appleton and Beynon (1948) using Slough ($\Phi = 51°$ N) data found the amplitude of lunar variation of foF2 to be 0·05 Mc/s and the maximum phase to be at 11 lunar hours, whereas for hpF2, they found corresponding values to be 2·0 km and 06 lunar hours. The variation at Huancayo as analysed by McNish and Gautier (1949) was different, the amplitude of lunar variation of noon foF2 being as high as 0·4 Mc/s (in sunspot minimum years 1941–44) with the maximum phase at 04 lunar hours. Thus the lunar variation near the geomagnetic equator was apparently higher in amplitude and nearly opposite in phase to that at higher latitudes. However, McNish and Gautier's result was obtained by using only noon values of foF2 while Martyn used the values at all hours. 04 lunar hours corresponds to nearly 4 days before the full-moon day. The occurrence of a phase opposition near the equator was corroborated by Osborne (1952) from his analysis of noon data (1949–51) of Singapore ($\Phi = 10·1°$ S). He found the noon

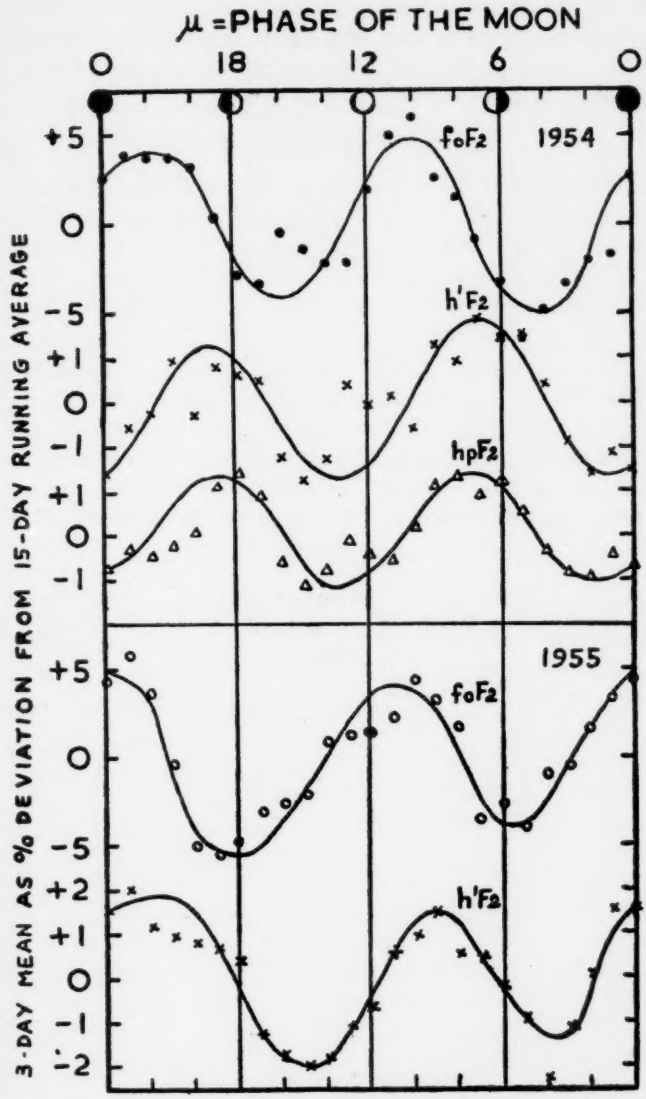

FIG. 1. Variation with lunar phase of midday foF2, hpF2 and h'F2 (10–14 hours) at Ahmedabad in 1954 and 1955.

maxima to occur about four days before full-moon and new-moon days, but the amplitude was slightly less than that at Huancayo. Bartels (1950)

confirmed the variations at Huancayo. His results were expressed as deviations from 27-day running averages. He found that the total change in foF2 due to lunar tide at noon in southern summer was 1·1 Mc/s while in southern winter, it was only 0·2 Mc/s.

ANALYSIS OF DATA AND RESULTS

In view of the above results, it was thought worthwhile to analyse the F2 data collected at Ahmedabad ($\Phi = 13{\cdot}6°$ N). The year 1954 was a minimum sunspot year with a mean sunspot number 4. As this year was almost free from magnetic disturbances, it was considered that 1954 data would be appropriate for analysis of lunar daily variation, when other influences were at a minimum. To start with, the analysis was made of midday foF2, h'f2 and hpF2, taken to be the mean of the values at 10–14 hours. The days in all the months having the same phase (μ) of the moon were grouped together and 24 such groups were obtained for the different phases of the moon. For each phase, the mean midday values (mean of the 5-hourly values at 10–14 hours) for the whole year was found. Whenever there was loss of record or blanketing by Es or failure of equipment, reasonable interpolation was made for the missing value. All the days for which data could be had were taken into account and seasonal changes were eliminated by taking yearly means. The results are given in Fig. 1, which clearly shows that the maximum amplitude occurs about 2 days after the full-moon and new-moon days for foF2 and about 5 days after full or new moon days for h'F2 and hpF2. The results are expressed as percentage deviations of 3-day mean centred at each lunar day from the 15-day running averages. Some points lie outside the curve and these are found to be just those for which the number of observations were few. In terms of lunar time, the phase of foF2 comes out to be 10 lunar hours and that for h'F2 and hpF2 about 07 lunar hours. The corresponding amplitudes are found to be about 4·5% in foF2 and about 1·7% in heights. The results for the year 1955 on the rising part of the solar cycle are shown in the same diagram. The maximum in 1955 has shifted earlier by a day compared to 1954, both in foF2 and h'F2. Fig. 2 gives the mean curves of lunar variation in foF2 and h'F2 for both the years together. The points for each year are marked differently. It will be seen that the phase agrees well with those observed at higher latitudes by Martyn, but the amplitude is larger. One reason for this may be that we have considered midday values only.

It was thought that it would be interesting to examine the lunar variation in foF2 at other Indian stations nearer the geomagnetic equator, *viz.*, Bombay, Madras and Tiruchirapalli. The midday values of foF2 for the year 1954

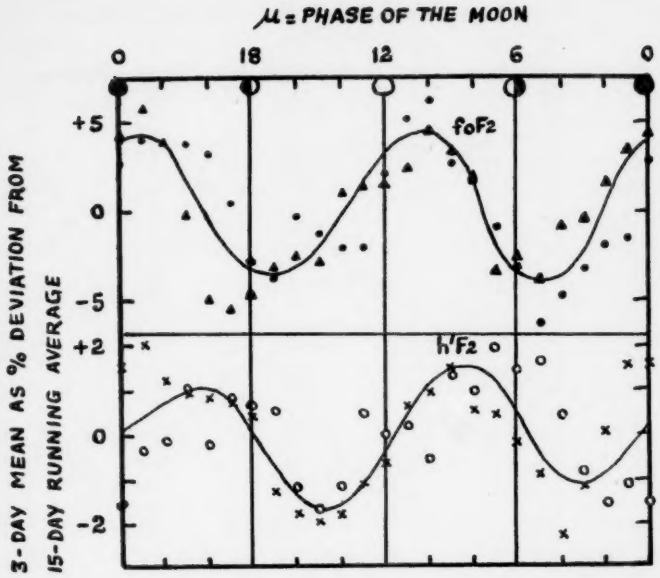

FIG. 2. Variation with lunar phase of midday foF2 and h'F2 (10–14 hours) at Ahmedabad in 1954–1955.

foF2: ···· 1954, ▲▲▲▲ 1955 ; h'F2: oooo 1954, xxxx 1955.

Full line curve is the mean for 1954–55.

at the above stations collected by All-India Radio were analysed in the same manner, and the results are given in Fig. 3. It is interesting to note that the phase at Bombay ($\Phi = 9{\cdot}5°$ N) is practically the same as at Ahmedabad, whereas at Madras ($\Phi = 3{\cdot}1°$ N), the phases are almost opposite. This shows that north of equator, a phase-reversal takes place somewhere between 9·5° N and 3·1° N geomagnetic latitude. Tiruchirapalli which is still near the equator has a maximum about 2½ days before full or new moon as against about 3½ days at Madras. Another point is that instead of an increase in amplitude towards the equator as observed by others, we find that the amplitude decreases after reaching a maximum. Observations at Ahmedabad were made with an automatic ionospheric recorder whereas at the other places they were made manually. The accuracy of reading in foF2 was 0·1 Mc/s at all the places.

It is interesting that although Bombay has nearly the same geomagnetic latitude to the north of the geomagnetic equator as Singapore is to the south, there is a difference between the lunar variations at the two places. While the equatorial type of variation is observed at Singapore, the middle

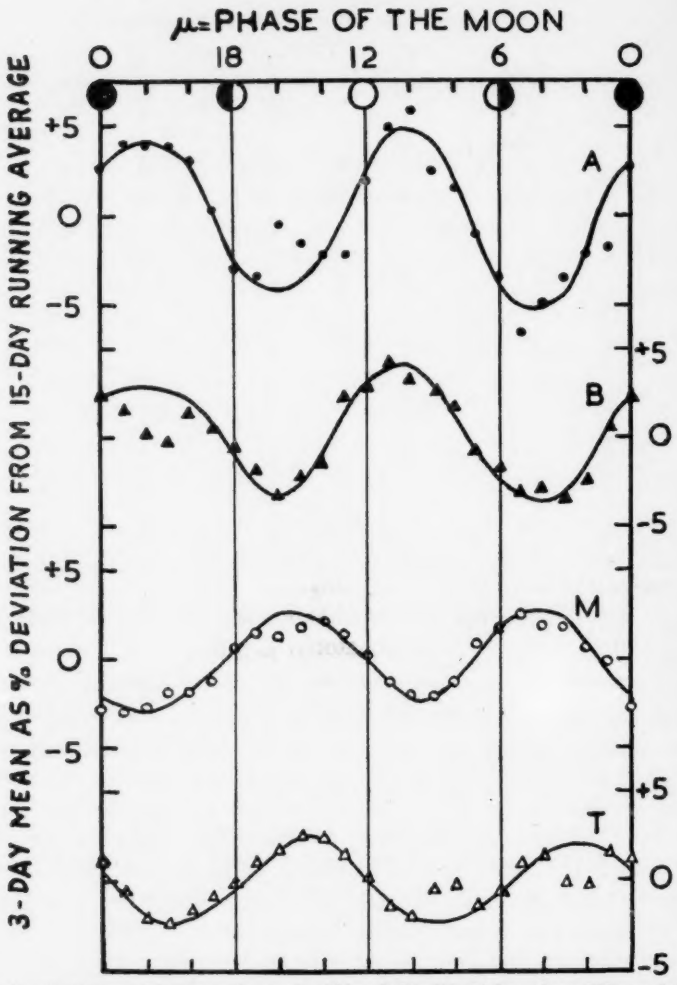

FIG. 3. Variation with lunar phase of midday foF2 (10–14 hours) at different latitudes in 1954. A: Ahmedabad, B: Bombay, M: Madras, T: Tiruchirapalli.

latitude type occurs at Bombay. The change to the equatorial type occurs between Bombay and Madras, perhaps nearer Bombay than Madras. Singapore is however only 1° 19′ north of the geographic equator.

To facilitate ready reference, the results of the analysis of the second harmonic components for 1954 are collected in Table I below; those of Singapore relate to 1948–51 and of Huancayo to 1941–44.

TABLE I

Amplitude P2 and Phase t2 of lunar Variation in foF2

Place	Geomag. lat.	foF2			hpF2	
		100P2 mean foF2	P2 Mc/s	t2 lunar hours	P2 km	t2 lunar hours
Ahmedabad ..	13·6° N	3·9	0·35	10·2	3·0	7·2
Bombay ..	9·5° N	2·6	0·24	10·0	..	..
Madras ..	3·1° N	1·8	0·14	3·8	..	..
Tiruchy ..	1·3° N	1·8	0·13	2·8	..	..
Huancayo ..	0·6° S	5·0	0·40	4·0	..	..
Singapore ..	10·1° S	(3·0)	(0·30)	(4·0)	..	..

The non-agreement of the results of Bombay and Singapore suggests that the lunar variation does not depend on geomagnetic latitude only. If we consider two stations according to geographical latitudes, Bombay (geogr. lat. 19° N) falls in the middle latitude group while Singapore (geogr. lat. 1·3° N) is in the equatorial group.

Bartels has shown that at Huancayo, the total change of noon foF2 during a lunar cycle in southern summer is nearly 5 times that in southern winter and Burkard (1951) has shown that the semidiurnal lunar variation of foF2 is pronounced during the daytime only and practically absent during the night. The significance of the phase-reversal of the lunar semidiurnal variation between the latitudes of Madras and Bombay and at some latitude to the south of Singapore remains to be explained. An analysis of the available Indian data to study the lunar variations in different seasons of the year is being undertaken.

REFERENCES

Appleton, E. V. and Beynon, W. J. G. — *Nature*, 1948, **162**, 486.

Bartels, J. .. *J. Atmosph. Terr. Phy.*, 1950, **1**, 2.

Burkard, O. .. *Ibid.*, 1951, **1**, 349.

Martyn, D. F. .. *Nature*, 1949, **163**, 34.

—— *et al.* .. *U.R.S.I. Special Report* No. 2 on 'Tidal Phenomena in the Ionosphere,' 1950.

McNish, A. G. and Gautier, T. N. — *J. Geoph. Res.*, 1949, **54**, 181.

Osborne, B. W. .. *Nature*, 1952, **169**, 661.

747-56. Prin galore Press Bangalore City, by C. Vasudeva Rao, Superintendent.
d by The Indian Academy of Sciences, Bangalore.

NOTICE TO AUTHORS

Scientific papers intended for publication in the *Proceedings of the Indian Academy of Sciences* can be accepted only when they are communicated by a Fellow of the Academy whose duty shall be to satisfy himself that such communications are fit to be read at the Meeting of the Academy and published in its *Proceedings*.

Papers should not ordinarily exceed fifty pages of foolscap. MSS. should be either typewritten or written in legible hand on one side of the paper. All papers should be carefully revised by the authors and should be absolutely in final form for printing. Position for text-figures should be indicated. Each paper shall conclude with a critical summary not exceeding 350 words.

Drawings, diagrams or other illustrations should be made on larger scale (preferably) twice the size than the ones in which they are intended to appear. They should be done in Indian ink on bristol board with lettering in pencil. Scale of magnification of camera lucida tracings should be indicated by the side of drawings. In certain special cases arrangements will also be made for monochrome lithographic and other colour plates. Reduction of illustrations desired should be indicated in pencil. Appropriate legends should accompany all drawings. Names of authors are to be marked in pencil on the left-hand corner of drawing sheets. Photomicrographs should be securely mounted with colourless paste.

All tables, quotations and footnotes which will be set hereafter (beginning from Vol. I, No. 2) in types smaller than the text, should be typewritten on separate sheets and placed with the text in proper sequence. Footnotes should be numbered in Arabic numerals.

References to literature in the text should be given, whenever possible, in chronological order, only the names of authors and years of publication, in brackets, being given. They should be cited in full after the summary, the authors' names following in alphabetical order. Thus,

Name or Names of author; Name of Journal (abbreviation) with a single underline; Year of publication; Number of Volume with a double underline, and lastly page. The following would be a useful illustration:—

Bergmann and Stather . . . . . Z. Physiol. Chem., 1926, 152, 189.

Two copies of slip-proof and wherever possible, a page proof for final revision will be sent to authors. All corrections are best made on the slip-proof which should be transmitted to the Office of the Academy. All proof corrections involve heavy expenses which would be negligible if the papers are carefully revised by the authors before submission.

Authors will be supplied with reprints of their papers at cost price, if intimation is given at the time of returning the slip-proof.

locks appearing in the *Proceedings* will be available for purchase by their tive authors. Orders for the same should be sent along with the corrected and in any case not later than one month after the date of publication paper. The price charged would be 25% of the actual cost of the blocks eight and despatching charges. If the blocks are reproduced in other ls or publications, due acknowledgment should be made in them to the *dings*.

e original drawings and plates of blocks appearing in the *Proceedings* returned to such of the authors as may require them provided the cost of hing such originals is borne by them.

CONTENTS

		PAGE
The Physics of Crystals	Sir C. V. Raman	32
On the Intensity and Polarisation of the Light from the Sky during Twilight—Part II.	J. V. Dave	336
Mineralogy of Some Indian Clays	M. Ramakrishna Rao	359
The Role of Solvent in Chemical Reactions. Part II. The Reaction between Aniline and Methyl Iodide in Different Solvents	V. S. Padmanabhan	368
Polarographic Behaviour of Metals in Ethanolamines. Part II. Cadmium	R. S. Subrahmanya	383
Variation with Lunar Phase of Midday Critical Frequencies and Heights of the F2 Layer over Ahmedabad and Other Low Latitude Stations	K. M. Kotadia and K. R. Ramanatha	